Discriminating Top-Antitop Resonances using Azimuthal Decay Correlations

Matthew Baumgart[1] and Brock Tweedie[2]

[1] *Department of Physics and Astronomy, Johns Hopkins University, Baltimore, MD 21218*
[2] *Physics Department, Boston University, Boston, MA 02215*

Top-antitop pairs produced in the decay of a new heavy resonance will exhibit spin correlations that contain valuable coupling information. When the tops decay, these correlations imprint themselves on the angular patterns of the final quarks and leptons. While many approaches to the measurement of top spin correlations are known, the most common ones require detailed kinematic reconstructions and are insensitive to some important spin interference effects. In particular, spin-1 resonances with mostly-vector or mostly-axial couplings to top cannot be easily discriminated from one another without appealing to mass-suppressed effects or to more model-dependent interference with continuum Standard Model production. Here, we propose to probe the structure of a resonance's couplings to tops by measuring the azimuthal angles of the tops' decay products about the production axis. These angles exhibit modulations which are typically $O(0.1\text{--}1)$, and which by themselves allow for discrimination of spin-0 from higher spins, measurement of the CP-phase for spin-0, and measurement of the vector/axial composition for spins 1 and 2. For relativistic tops, the azimuthal decay angles can be well-approximated without detailed knowledge of the tops' velocities, and appear to be robust against imperfect energy measurements and neutrino reconstructions. We illustrate this point in the highly challenging dileptonic decay mode, which also exhibits the largest modulations. We comment on the relevance of these observables for testing axigluon-like models that explain the top quark A_{FB} anomaly at the Tevatron, through direct production at the LHC.

I. INTRODUCTION

New resonances that decay to $t\bar{t}$ are a common feature of many models of physics beyond the Standard Model (SM). Indeed, top's unusually large coupling to the electroweak sector is often taken as a hint of some special role in TeV-scale physics.

Recently, another hint has arisen at the Tevatron, in the measurement of a 3.4σ anomaly in the top pair forward-backward asymmetry (A_{FB}) at high invariant mass [1] (as well as lower-significance biases of the same sign observed in [2–4], and more recently in the dileptonic mode [5]). One possible explanation of this effect is the presence of an s-channel $q\bar{q} \to t\bar{t}$ resonance somewhere beyond the Tevatron's direct discovery reach, which is interfering with the SM production. As argued in [6], a straightforward model framework which can lead to the required interference is a color octet spin-1 boson with sizable axial couplings (of opposite sign) to light quarks and tops; e.g., some variant of a heavy axigluon [7–9].

Such a resonance should be visible at the LHC, even if it turns out to be very broad, and likely even in the upcoming 7 TeV run [10–13]. This discovery would already be extremely suggestive. Direct confirmation of A_{FB}-related effects may also be possible, despite the fact that the pp initial state is forward-backward symmetric [11, 14–17]. However, fully establishing the connection between the resonance and A_{FB} will benefit from independent measurements of the resonance's chiral couplings to top quarks and light quarks, which will necessarily involve additional detailed kinematic analyses both on- and off-peak [18–22]. Most of these analyses exploit effects that, like A_{FB} itself, arise from interference with QCD.

Motivated by this endeavor, but also with an eye toward more general models, we can consider the following question: Given that a resonance (either a peak or high-mass excess) is discovered in the $m_{t\bar{t}}$ spectrum at the LHC, how much can we directly learn about the chiral structure of its couplings to tops without relying on more model-dependent QCD interference effects? In particular, in the case of a spin-1 resonance, could we determine if it couples to tops mostly-axially by using only on-peak observables?

Of course the presence of a large axial component could be readily established if the individual chiral couplings are highly biased toward left-handed or right-handed. At energies well above $2m_t$, the different chiralities map almost uniquely onto distinct top helicities, which can be discriminated by studying the rest frame decay angles of individual tops [23, 24]. The differences are also encoded in the lab-frame energies of the leptons and b-jets relative to the top and to each other [25–27], as well as in the energy sharing between the jets (or subjets) in hadronic decay [28].

The situation becomes more subtle if the couplings to the two top chiralities are more democratic. Single-side spin analysis then becomes inadequate to accurately probe the relative magnitudes between vector and axial couplings, and we must incorporate measurements of spin correlations between the two sides of the event. These correlations are affected by the interference between the different helicity production modes, and can be used to directly

probe the *signed* ratio of top's chiral couplings. Nonetheless, the most commonly used top spin-correlation variables [29–34] (reviewed in [23, 35]) are largely insensitive to helicity interference for heavy spin-1 resonances, and generally involve complicated reconstructions that are not obviously ideal for fast-moving tops. Our main aim in this paper is to demonstrate how to construct simple observables that *are* sensitive, as well as straightforward to measure.

For spin-1 resonances well above $2m_t$, the on-peak helicity interference is most directly encoded in the azimuthal distributions of the tops' decay products about the $t\bar{t}$ production axis. This is quite analogous to the effect measured at LEP in $Z \to \tau^+\tau^-$ [36–39]. It is also closely related to the observables explored in [40–44], which use the same type of interference as a probe of the spins of new pair-produced particles, or particles that are singly-produced in association with a jet. We now assume that we know the spin of the top quark, and use the interference to tell us about how it was produced.[1] As is typical for top spin observables, the decay product most sensitive to the correlation is the charged lepton, and we focus here on the dileptonic decay mode. We also emphasize that the same effects occur in the ℓ+jets mode, though with smaller amplitude. We will show that the dileptonic azimuthal distributions can be measured at the LHC, even given the usual kinematic difficulties, and even using very minimalistic reconstruction strategies. These distributions exhibit surprisingly robust modulations at the 30-40% level for pure vector or axial coupling, but with opposite signs.

Our observations also generalize beyond spin-1 resonances. The minimal couplings to spin-2 have a similar chiral structure, which will be amenable to the same style of analysis. Spin-0 resonances near $t\bar{t}$ threshold have been a topic of detailed study for the past two decades, due to the possibility of detecting scalars from the Higgs-sector via gluon fusion (e.g. [46, 47]). Variables sensitive to the scalar/pseudo-scalar composition have therefore been known for a long time. However, we will emphasize that azimuthal correlations make this composition visible in a very transparent way, especially if the resonance is heavy. They also allow for a straightforward determination of whether a resonance is spin-0 versus higher spin, independent of $t\bar{t}$ polar decay angle correlations or the production angle distribution. Given the large amount of easily-measured information made available to us through these correlations, we highly advocate incorporating them into the set of $t\bar{t}$ resonance discrimination observables laid out in [23].

In the next section, we discuss the angular spin-correlation observables. We start by reviewing the basic formalism, and then proceed to the details particular to spin-0, spin-1, and spin-2. In particular, our discussions of spin-1 and spin-2 demonstrate how vector-coupled and axial-coupled resonances can be distinguished from each other with azimuthal correlations, as well as from spin-0. In Section III we demonstrate that our observables should be accessible experimentally in the dileptonic channel. We estimate the amount

---

[1] See also [45] for a study using the individual top decay azimuthal angles to probe new $t\bar{t}$ production contributions at an ILC.

of cross section required to be able to distinguish between pure vector and axial-vector at early- and late-stage LHC, and discuss possible relevance to the Tevatron top A_{FB} anomaly. We conclude in Section IV. The Appendices include complete formulas for leading-order, on-peak $t\bar{t}$ production and decay angular distributions for resonances up to spin-2.

II. SPIN CORRELATIONS

After a heavy resonance decays to a pair of top quarks, the tops themselves decay into $b\ell^+\nu$ or $bq\bar{q}'$ through an on-shell W boson. In general, a given 6-body final-state kinematic configuration could be produced by a number of intermediate top/anti-top spin configurations. Since we never measure the tops' spins, these different spin channels coherently interfere with one another, leading to distinctive imprints on the final-state angular distributions.

The relevant behavior of the top decay matrix elements becomes transparent when we exploit a fortuitous simplification. If we look at the 3-body semileptonic top decay amplitude at leading-order, stripping off the W propagator, we can Fierz down to

$$\mathcal{M}(t \to b\ell^+\nu) \propto \left(u(t)_L^T \, \epsilon \, v(\ell)_L\right) \left(u(b)_L^\dagger \, \epsilon \, u(\nu)_L^*\right), \tag{1}$$

where u's and v's represent the spinor polarizations, and we have kept only the two components from left-chirality. Given a specific top spin and decay configuration, we can map out how the amplitude changes as we rotate the decay products in the top rest frame. Because the b-quark and neutrino factorize off into a rotationally-invariant product, the angular dependence of the amplitude is determined exclusively by the direction of the lepton:

$$\mathcal{M}(t_\uparrow \to b\ell^+\nu) \propto e^{i\phi_\ell/2} \cos\frac{\theta_\ell}{2}$$
$$\mathcal{M}(t_\downarrow \to b\ell^+\nu) \propto e^{-i\phi_\ell/2} \sin\frac{\theta_\ell}{2}, \tag{2}$$

where we are using a standard right-handed coordinate system with spin quantized along the z-axis. If we instead decay an anti-top, we simply swap $\cos \leftrightarrow \sin$. (The same formulas also hold with $\ell \to d/s$ in fully hadronic decay.) Notably, the phases of the amplitudes depend on the azimuthal angle of the lepton about the top's spin vector.

Since we are ultimately interested in resonances beyond the Tevatron reach, and well-above top threshold, we will restrict our discussions to the chiral production limit. (More complete formulas, valid down to threshold, appear in the Appendices.) In this limit, the most natural spin basis is the helicity basis. We therefore quantize spin along the top/anti-top production axis in the $t\bar{t}$ CM frame, and measure ϕ around this axis (the "azilicity angle," in the terminology of [48]). By convention we choose $+z$ to point along the t direction. This may differ with conventions used in other places, where the $\bar{t}$ decay coordinate system is independently defined with respect to its own direction of flight. To define the x- and y-axes,

3

we use the beams. We can construct $\hat{y}$ by crossing the t direction with one of the beam directions, so that it points out of the $t\bar{t}$ production plane. (The ambiguity over which beam to pick at the LHC will not be important for our purposes.) The $\hat{x}$ direction is then defined as usual for a right-handed coordinate system, as $\hat{y} \times \hat{z}$. Consequently, when we measure ϕ angles about the production axis, we define $\phi = 0$ to lie in the production plane. This is, of course, our only physically-motivated choice.[2] Finally, we construct the individual top and anti-top decay coordinate systems by actively boosting the tops to rest (without rotation) along the production axis, and measuring all angles in this common reference frame.

Assembling a complete 6-body decay matrix element for a hypothetical heavy particle ("X") is now straightforward. Taking the narrow width approximation, and implicitly picking some definite initial spin state, we can write

$$\mathcal{M}_{\text{tot}} = \sum_{a,\bar{a}} \mathcal{M}(X \to t_a \bar{t}_{\bar{a}}) \mathcal{M}(t_a \to b\,\ell^+ \nu) \mathcal{M}(\bar{t}_{\bar{a}} \to \bar{b}\,\ell^- \bar{\nu}), \tag{3}$$

where a and $\bar{a}$ label the spin of the top and anti-top, respectively. For spin-0 resonances, the tops are forced to have opposite spins (identical helicities). In the chiral limit, tops from a heavy spin-1(2) decay will have identical spins (opposite helicities). The matrix elements schematically reduce to

$$\mathcal{M}_{\text{tot}}(X_0 \to b\,\ell^+ \nu \bar{b}\,\ell^- \bar{\nu}) \sim \mathcal{M}(X_0 \to t_\uparrow \bar{t}_\downarrow)\, e^{i(\phi_\ell - \overline{\phi}_\ell)/2} \cos\frac{\theta_\ell}{2} \cos\frac{\overline{\theta}_\ell}{2} \;+$$

$$\mathcal{M}(X_0 \to t_\downarrow \bar{t}_\uparrow)\, e^{-i(\phi_\ell - \overline{\phi}_\ell)/2} \sin\frac{\theta_\ell}{2} \sin\frac{\overline{\theta}_\ell}{2}$$

$$\mathcal{M}_{\text{tot}}(X_{1(2)} \to b\,\ell^+ \nu \bar{b}\,\ell^- \bar{\nu}) \sim \mathcal{M}(X_{1(2)} \to t_\uparrow \bar{t}_\uparrow)\, e^{i(\phi_\ell + \overline{\phi}_\ell)/2} \cos\frac{\theta_\ell}{2} \sin\frac{\overline{\theta}_\ell}{2} \;+$$

$$\mathcal{M}(X_{1(2)} \to t_\downarrow \bar{t}_\downarrow)\, e^{-i(\phi_\ell + \overline{\phi}_\ell)/2} \sin\frac{\theta_\ell}{2} \cos\frac{\overline{\theta}_\ell}{2}, \tag{4}$$

with the bar indicating the anti-top (ℓ^-) decay angle. The final rate will therefore contain modulating terms dependent on $\phi_\ell \pm \overline{\phi}_\ell$, with phase or magnitude dependent on the complex production matrix elements. For the case of spin-0, which modulates as $(\phi_\ell - \overline{\phi}_\ell)$, the two X_0 decay elements are conjugates of each other. Consequently, the modulation is subject to a pure phase offset, where phases differing from 0 or π signal CP-violation. For spin-1 and spin-2, which modulate as $(\phi_\ell + \overline{\phi}_\ell)$, the effect is instead pure magnitude, varying with the signed ratio of chiral couplings. (E.g., in the case of purely LH or RH chiral production, there is only one helicity channel, and therefore no modulation effect.) Since we will consider scenarios where X is a singly-produced resonance, and not necessarily extremely narrow, there may also be contributions to the azimuthal modulations from interference with the

---

[2] In the presence of nonvanishing $t\bar{t}$ system p_T, we must be somewhat careful when performing this coordinate construction, as the beams are not necessarily aligned in the $t\bar{t}$ CM frame. We address this issue in Section III.

SM. Still, the effect tends to be subleading for resonances with a well-defined peak. We discuss the issue in more detail at the end of Appendix B.

We can also see similar correlations between *any* two decay products, one from the top side and one from the anti-top side. While Eq. 1 naively suggests no dependence on the b-quark and neutrino directions, these are still highly kinematically correlated with the lepton via the (approximately) fixed mass of the W boson and overall four-momentum conservation for the top. Integrating out the phase space of all but one particle on each side of the event leaves over angular correlations that are essentially identical in structure to the double-lepton correlations, including phase information. The correlations simply scale with constant spin analyzing powers associated to each particle species: 1 for leptons, -0.3 for neutrinos, -0.4 (+0.4) for b-quarks (W-bosons), and 0.5 for the softer of the two W decay products in the top rest frame [49]. The effects which we seek to exploit are maximal for leptons, but could also be measured in principle by including b-jets or jets from the W decay. (Indeed, formulas analogous to Eq. 4, but instead using W-bosons, appeared long ago in [31] in the context of spin correlations between top pairs at the SSC.)

Here, we focus on the double-lepton correlations, and therefore the dileptonic $t\bar{t}$ decay channel. This maximizes the azimuthal modulation effects and is the least susceptible to reducible backgrounds. However, it also has the lowest rate (5%, versus 30% for ℓ+jets), and suffers from kinematic reconstruction difficulties due to the two approximately back-to-back neutrinos. We address the latter difficulty in Section III. Incorporating the ℓ+jets mode will also be very important, even though the modulations will be smaller in amplitude (e.g., 40% if we correlate a lepton with a b-quark or W-boson from the other side of the event). We reserve a detailed exploration for future work, but include some commentary.

In what follows, we will usually be integrating out all but one or two angular variables, only restoring the full (and usually very complicated) correlated angular dependence in the Appendices. Much of the discussion will parallel that of [23], which comprehensively studied some of the standard correlation observables in the context of resonance discrimination for arbitrary spins. We also note that more sophisticated analyses, such as the likelihood approach of [50, 51], could potentially distinguish the different resonance scenarios even more efficiently.

A.   Spin-0

We begin with the well-studied example of a spin-0 resonance. Single-production of such a resonance is typically chirality-suppressed from a $q\bar{q}$ initial state, and dominantly proceeds through heavy quark loops in gluon fusion. It is therefore perhaps nongeneric for this process to have a healthy rate above backgrounds when the resonance mass is at or above a TeV. However, independent of any model-building concerns, at a minimum, spin-0 serves as both an illustrative example of our methods and as a baseline hypothesis against

which any higher-spin resonances must be tested.

At dimension-four, an arbitrary scalar coupling to $t\bar{t}$ is made of a linear combination of CP even and odd pieces,

$$\mathcal{L}_{\text{int}} = -\phi^a \, \bar{t}^i \, (y + i\,\tilde{y}\,\gamma_5) \, T^a_{ij} t^j, \tag{5}$$

where T^a_{ij} is the color matrix appropriate to the scalar's representation (singlet or adjoint). The dependence on the scalar's color factorizes, so we ignore it in the remainder of the discussion. Since our interest is in the different top helicity components, we can rewrite Eq. 5 in the chiral field basis,

$$\mathcal{L}_{\text{int}} \to -y\,\phi \left(e^{i\,\alpha}\,\bar{t}_R t_L \, + \, e^{-i\,\alpha}\,\bar{t}_L t_R \right), \tag{6}$$

where $y\,e^{i\,\alpha} \equiv y - i\,\tilde{y}$. Since the $t\bar{t}$ pair can have no angular momentum along their production axis, only same-helicity tops are created in the scalar decay. In the chiral limit, the production matrix elements differ only by the overall phase factor $e^{\pm i\,\alpha}$. The angle α is equal to 0 for a CP-even scalar and $\pi/2$ for a pseudoscalar.

Squaring $\mathcal{M}_{\text{tot}}$ in Eq. 3 and integrating over phase space except for lepton orientations,

$$\frac{d^4\Gamma}{d\Omega_\ell \, d\bar{\Omega}_\ell} \propto 1 + \cos\theta_\ell \cos\bar{\theta}_\ell - \sin\theta_\ell \sin\bar{\theta}_\ell \cos\left(\phi_\ell - \bar{\phi}_\ell + 2\alpha \right). \tag{7}$$

Getting the distribution of polar angles is trivial from this equation, as either lepton's azimuthal integral will kill the last term. This leaves over the well-known formula

$$\frac{d^2\Gamma}{d\cos\theta_\ell \, d\cos\bar{\theta}_\ell} \propto 1 + \cos\theta_\ell \cos\bar{\theta}_\ell. \tag{8}$$

The prefactor of the double-cosine term is characteristic of a scalar, and has been advocated for distinguishing the overall spin of a resonance [23] (though, we re-emphasize, typically with a coordinate change $\bar{\theta}_\ell \to \pi - \bar{\theta}_\ell$). However, we see that dependence on the phase of the coupling has dropped out. To retain it, a traditional approach is to instead integrate out all angles except for the 3D opening angle between the leptons, which we call χ.[3] Recall that we have actively boosted both tops along the production axis into their respective rest frames, and then defined a common coordinate system with the z-axis given by the t direction. It is in these coordinates where we measure χ. We get a simple linear dependence on $\cos\chi$,

$$\frac{d\Gamma}{d\cos\chi} \propto 1 + \frac{1 - 2\cos(2\alpha)}{3} \cos\chi. \tag{9}$$

A CP-even scalar has a different slope compared to a pseudoscalar, $-\frac{1}{3}$ vs. $+1$, making the distinction between the two straightforward in principle, provided that one can fully reconstruct the individual top quark rest frames. Such a reconstruction can be challenging.

---

[3] Elsewhere in the literature this has been called ϕ. We relabel it to avoid confusion.

However, as shown in [52], the resolution on the opening angle may still be good even for highly boosted dileptonic top pairs. A more fundamental issue, as we will see in the next subsection, is that spin-1 and spin-2 resonances all look identical to the CP-even scalar (and to each other) when using this angle.

A more straightforward way to maintain the α-dependence, without needing polar angles, is to integrate Eq. 7 over all angles except for the ϕ offset between the leptons. This gives a modulating distribution

$$\frac{d\Gamma}{d(\phi_\ell - \bar\phi_\ell)} \propto 1 - \left(\frac{\pi}{4}\right)^2 \cos(\phi_\ell - \bar\phi_\ell + 2\alpha), \tag{10}$$

with a sizable amplitude of roughly 60%. We see that the modulation flips sign as we go from CP-even scalar ($\alpha = 0$) to pseudoscalar ($\alpha = \pi/2$), and that the magnitude of the modulation is the same $O(1)$ size for any admixture. Since ϕ_ℓ and $\bar\phi_\ell$ are boost-invariant along the individual tops' directions of motion in the $t\bar t$ CM frame, using Eq. 10 may be amenable to simpler $t\bar t$ reconstruction methods that do not necessarily need accurate information about the tops' velocities. Moreover, as we will see below, the equivalent distributions for spin-1 and spin-2 resonances are flat, breaking the degeneracy with the CP-even scalar, and already allowing a significant degree of spin discrimination in this variable alone.

B. Spin-1

We can write out the generic dimension-four coupling between a spin-1 resonance and a $t\bar t$ pair as

$$\mathcal{L}_{\rm int} = A_\mu^a \bar t^i \left(g_V + g_A \gamma^5\right) \gamma^\mu T_{ij}^a t^j, \tag{11}$$

where g_V and g_A are real numbers. Again, we will suppress color in what follows, and go over to the chiral field basis,

$$\mathcal{L}_{\rm int} \to A_\mu \left(g_L \bar t_L \gamma^\mu t_L + g_R \bar t_R \gamma^\mu t_R\right). \tag{12}$$

Unlike the couplings of a scalar, these couplings preserve chirality, and they differ in magnitude and sign instead of being complex conjugates of each other. For convenience, we define a coupling angle ξ,

$$\begin{aligned} g_L &= g\cos\xi \\ g_R &= g\sin\xi. \end{aligned} \tag{13}$$

Our decay angular distributions will be functions of ξ, with the overall g factored out. By imposing symmetry under parity, we can have the special cases of $g_L = g_R$ (true vector, $\xi = \pi/4$) or $g_L = -g_R$ (axial-vector, $\xi = 3\pi/4$). We are particularly interested in finding observables that discriminate between these two cases.

We again assume the chiral limit for top production, setting $m_t = 0$ in the decay matrix element of the heavy resonance. The finite-mass effects in the angular distributions can in fact be different for the true vector and the axial-vector, in principle providing additional means of discrimination if the resonance is light enough.[4] However, by focusing on the features of the angular correlations that are asymptotically insensitive to m_t/M, our observations here will be robust up to arbitrarily high resonance masses.

We begin our discussion of spin-1 angular distributions by looking at the standard double-cosine distribution, integrating over all other angles,

$$\frac{d^2\Gamma}{d\cos\theta_\ell \, d\cos\bar{\theta}_\ell} \propto 1 + \cos(2\xi)\left(\cos\bar{\theta}_\ell - \cos\theta_\ell\right) - \cos\theta_\ell \, \cos\bar{\theta}_\ell. \qquad (14)$$

This is the direct analog of Eq. 8 in the spin-0 case. The first term signals parity violation, and is only active if the resonance is neither pure vector nor pure axial-vector. (Note that $\cos(2\xi) = (g_L^2 - g_R^2)/(g_L^2 + g_R^2)$.) As discussed in the introduction, a large chirality bias could be established already with single-side angular distributions, such as $d\Gamma/d\cos\theta_\ell$, and the construction of the double-cosine distribution then essentially serves only as a cross check. Incidentally, this observation by itself would already disfavor a spin-0 interpretation. On the other hand, in the more chirality-symmetric case ($\cos(2\xi) \simeq 0$, $|g_L| \simeq |g_R|$), the correlated distribution becomes more useful, as the sign of the double-cosine term is opposite that for the scalar. This is a direct indication that the tops are coming out in a same-spin (opposite-helicity) configuration, again disfavoring spin-0 [23]. Crucially, however, all terms in the distribution are insensitive to the relative sign between the chiral couplings, up to the finite-mass corrections mentioned above. Consequently, it will likely be quite difficult to tell whether the resonance is vector-coupled or axially-coupled using only the double-cosine distribution.

Turning to the distribution over the 3D lepton angle χ does not help. It is

$$\frac{d\Gamma}{d\cos\chi} \propto 1 - \frac{1}{3}\cos\chi, \qquad (15)$$

independent of ξ. This is identical to the CP-even scalar distribution, Eq. 9, again up to the small $(m_t/M)^2$ corrections which we have neglected. We therefore learn very little from this distribution if we are interested in the properties of spin-1 resonances.

To robustly determine the signed ratio of chiral couplings, we again suggest the alternative tactic of focusing on the lepton azimuthal angles with respect to the production axis. There are now three major differences with the spin-0 case. First, as indicated in Eq. 4, the

---

[4] In particular, the double-cosine distribution for spin-1 resonances in the $t\bar{t}$ threshold limit is quite different between the two cases. An axial-vector has a relative double-cosine coefficient of -1 for all values of m_t/M, whereas a true vector's relative coefficient approaches -1/3 at threshold (*cf.* Eq. B3). In contrast, for a 1 TeV resonance, the coefficients differ from each other by only about 10%, and the discrepency shrinks like $(m_t/M)^2$. Similar conclusions also hold for the $\cos\chi$ distribution, though the finite-mass effects there might be easier to measure since the distribution is one-dimensional instead of two-dimensional.

modulation switches from $(\phi_\ell - \bar{\phi}_\ell)$ to $(\phi_\ell + \bar{\phi}_\ell)$, and therefore now refers to the orientation of the production plane (zx-plane).[5] This is a consequence of the fact that the spin-1 resonance carries a polarization which is necessarily fully correlated with the beams. The second difference is that the coupling angle ($\alpha \to \xi$) now affects the modulation's amplitude, not its phase. The third difference, which also follows from nonzero polarization, is that the decay angle distributions can become correlated with the $t\bar{t}$ production angle, which we call Θ. In what follows, we will implicitly average between rates at Θ and $\pi - \Theta$, so that effectively $\Theta \in [0, \pi/2]$.

For a resonance produced in $q\bar{q}$ annihilation, the component of the resonance's spin along the beam is $J_{\text{beam}} = \pm 1$, and the joint production/azimuthal angle distribution is

$$\frac{d^2\Gamma_{J_{\text{beam}}=\pm 1}}{d(\phi_\ell + \bar{\phi}_\ell)\, d\cos\Theta} \propto \left(1 + \cos^2\Theta\right) - \left(\frac{\pi}{4}\right)^2 \sin(2\xi)\sin^2\Theta \cos(\phi_\ell + \bar{\phi}_\ell). \tag{16}$$

Unlike the double-cosine distribution, which depends only on $\cos(2\xi)$, the azimuthal modulation depends on $\sin(2\xi) = 2g_L g_R/(g_L^2 + g_R^2) = 2/(g_L/g_R + g_R/g_L)$, and hence is directly sensitive to the signed ratio g_L/g_R. Perhaps fortunately, the modulation is largest for central production, which is the easiest case to reconstruct in real detectors. (The modulation shuts off for $t\bar{t}$ produced along the beam, since only one helicity state can contribute.) Fully integrating out the production angle, the distribution reduces to

$$\frac{d\Gamma_{J_{\text{beam}}=\pm 1}}{d(\phi_\ell + \bar{\phi}_\ell)} \propto 1 - \frac{1}{2}\left(\frac{\pi}{4}\right)^2 \sin(2\xi)\cos(\phi_\ell + \bar{\phi}_\ell), \tag{17}$$

which is very similar to the spin-0 ϕ-*difference* distribution, Eq. 10. However, it is straightforward to see that, respectively, a spin-1 resonance is non-modulating over $(\phi_\ell - \bar{\phi}_\ell)$,[6] whereas a spin-0 resonance is non-modulating over $(\phi_\ell + \bar{\phi}_\ell)$. Using *both* of these distributions can therefore tell us quite a lot about both the spin of the resonance and its coupling structure, independent of any other measurements such as the production angle distribution (trivial for spin-0 but nontrivial for spin-1), or observables incorporating the tops' polar decay angles (sensitive to chirality biases).

We can also give the analogue of Eq. 16 for a resonance with $J_{\text{beam}} = 0$. Such a state would come from gluon fusion and is typically suppressed, partly because the gluon parton luminosities drop very quickly with energy, and partly because the required gauge-invariant operators are dimension-six.[7] We include this case for completeness, and since it is still possible that the light quark couplings are highly suppressed, making this the dominant production mode. The production/azimuthal angle distribution becomes

$$\frac{d^2\Gamma_{J_{\text{beam}}=0}}{d(\phi_\ell + \bar{\phi}_\ell)\, d\cos\Theta} \propto \sin^2\Theta \left[1 + \left(\frac{\pi}{4}\right)^2 \sin(2\xi)\cos(\phi_\ell + \bar{\phi}_\ell)\right]. \tag{18}$$

---

[5] One way to picture the construction of $(\phi_\ell + \bar{\phi}_\ell)$ is as follows. Reflect the ℓ^- in the $t\bar{t}$ production plane, thereby flipping the sign of its ϕ angle. Then take the difference in ϕ as before.

[6] This modulation is generically induced by nonzero m_t effects (*cf.* Eq. B5).

[7] Note that the Landau-Yang theorem [53, 54] forbids production of a color-singlet spin-1 resonance through gluon fusion. Implicitly, we only consider color octet resonances.

We see that the modulation persists, but it is now factorized from the production angle and is consequently twice as large when Θ is integrated out. It also has the opposite sign. While this change in sign and magnitude could certainly lead to confusion over the true value of g_L/g_R, the production angle distribution is nonetheless still quite distinct, allowing an experimentally-driven determination of whether a $J_{\text{beam}} = 0$ or a $J_{\text{beam}} = \pm 1$ interpretation is appropriate.

C. Spin-2

Like spin-1, spin-2 particles can couple with different magnitudes to left and right-handed tops (and other fermions), though the leading interaction is now dimension-five,

$$\mathcal{L} \propto \frac{\cos \xi}{\Lambda} h^{\mu\nu} \left(\bar{t}_L (i \overleftrightarrow{D}_\nu) \gamma_\mu t_L \right) + \frac{\sin \xi}{\Lambda} h^{\mu\nu} \left(\bar{t}_R (i \overleftrightarrow{D}_\nu) \gamma_\mu t_R \right), \tag{19}$$

where h is a traceless and symmetric rank-2 tensor field, and Λ is the heavy scale that controls the strength of the operator. (This coupling is for a color-singlet field, but for color-octet we need only a trivial color matrix insertion.) Once again, we can build the traditional observables and see that they tell us nothing about the relative sign between left and right-handed couplings. (The double-cosine distributions and $\cos \chi$ distributions are identical to spin-1.) Just as with the other spins, the azimuthal angle distributions preserve this information.

Quite analogous to spin-1, the top production and decay angle distributions are correlated with each other. To get the equivalent of Eq. 16, we must replace

$$1 + \cos^2 \Theta \rightarrow 1 - 3 \cos^2 \Theta + 4 \cos^4 \Theta$$
$$\sin^2 \Theta \rightarrow - \left(1 - 5 \cos^2 \Theta + 4 \cos^4 \Theta \right). \tag{20}$$

The coefficient of the modulating term now goes through a zero at $\cos \Theta = 0.5$. Integrating over production angles, the modulation is diluted with respect to spin-1 by a factor of three (and flipped in sign),

$$\frac{d\Gamma_{J_{\text{beam}}=\pm 1}}{d(\phi_\ell + \bar{\phi}_\ell)} \propto 1 + \frac{1}{6} \left(\frac{\pi}{4} \right)^2 \sin(2\xi) \cos(\phi_\ell + \bar{\phi}_\ell). \tag{21}$$

While the production angle distribution is potentially a giveaway that the resonance is spin-2, the reduced $(\phi_\ell + \bar{\phi}_\ell)$ modulation will make discrimination of the top couplings much more difficult. However, given adequate statistics, focusing on the region of central production would allow a much larger modulation to be seen.

A spin-2 resonance can also be produced in gluon fusion, also through dimension-five operators. This can in principle lead to both $J_{\text{beam}} = \pm 2$ and $J_{\text{beam}} = 0$, but the latter

production mode is in fact absent at dimension-five.[8] We therefore exclusively focus on $J_{\text{beam}} = \pm 2$. (We include $J_{\text{beam}} = 0$ in our discussions in Appendix C, as it may still arise from yet higher-dimension operators.) The production angle no longer factorizes out, and we are left with a joint production/azimuthal angle distribution much like Eq. 16, but with an additional overall factor of $\sin^2 \Theta$. Since the production is biased more centrally, where the modulation is largest, the Θ-integrated modulation is now *enhanced*,

$$\frac{d\Gamma_{J_{\text{beam}}=\pm 2}}{d(\phi_\ell + \bar\phi_\ell)} \propto 1 - \frac{2}{3}\left(\frac{\pi}{4}\right)^2 \sin(2\xi)\cos(\phi_\ell + \bar\phi_\ell). \tag{22}$$

Similar to the spin-1 case, gluon fusion leads to larger modulations with opposite sign. Again, distinguishing between $q\bar{q}$ and gg (as well as spin-1 in any production mode) is possible in principle by studying the Θ distribution.

III. OBSERVING AZIMUTHAL CORRELATIONS AT THE LHC

We now turn to the question of whether the azimuthal modulations discussed in Section II are actually observable at the LHC, and in what cases we might be able to discriminate between different resonances. We focus on the dileptonic mode, which has the largest azimuthal correlation effects amongst $t\bar{t}$ decay modes, but which also has the lowest branching fraction and, more pressingly, the fewest number of visible decay products. Given the presence of *two* experimentally-invisible neutrinos, it is fair to ask 1) whether the resonance can be identified, and 2) whether the azimuthal observables discussed above can be reliably reconstructed. We address these two concerns in turn, in the context of simple LHC simulations that include showering/hadronization, gaussian energy smearing, and basic analysis cuts. As described in more detail in the subsections below, we find that minimalistic strategies work quite well, and that the modulations are very robust.

A. Simulation and basic event selection in the dileptonic mode

We generate 6-body dileptonic resonance and background samples at leading-order, with full angular correlations, using `MadGraph/MadEvent v4.4.51` [55] and its topBSM [23]

---

[8] For color singlet spin-2, the interaction $h_{\mu\nu}\text{Tr}(G^{\mu\alpha}G_\alpha^\nu)$, where G is the gluon field-strength, contains no coupling to the $J_{\text{beam}} = 0$ state on-shell. We could instead try to couple through the parity-odd interaction $h_{\mu\nu}\text{Tr}(G^{\mu\alpha}\tilde{G}_\alpha^\nu)$, but this vanishes identically when $h_{\mu\nu}$ is traceless. Considering an octet resonance, our only options are $\text{Tr}(h_{\mu\nu}\{G^{\mu\alpha}, G_\alpha^\nu\})$ or $\text{Tr}(h_{\mu\nu}[G^{\mu\alpha}, \tilde{G}_\alpha^\nu])$, each of which also lead to vanishing amplitude for $J_{\text{beam}} = 0$.

model.[9] We subsequently shower/hadronize with `PYTHIA 6.4` [56] and cluster the resulting particles into jets with `FastJet v2.4.2` [57] without detector simulation. We then apply gaussian energy smearings $\sigma(E)/E$ to the jets $(5.6\,\mathrm{GeV}/E \oplus 1.25\sqrt{\mathrm{GeV}/E} \oplus 0.033)$, electrons (0.02), and muons $(0.05 \times \sqrt{E/\mathrm{TeV}})$.

For very energetic tops, the lepton may be separated from the b-jet by a fairly small angle, possibly failing ordinary isolation criteria and subjecting us to semileptonic heavy flavor backgrounds. Nonetheless, these leptons can probably be reliably discriminated using tracker-level "mini-isolation" criteria with shrinking cones [58, 59], or through a number of other simple means [60, 61]. We accept into our analysis events with exactly two opposite-signed leptons (electrons or muons) that pass mini-isolation as described in [58], and with $p_T > 20$ GeV and $|\eta| < 2.5$. This set of cuts (or some modest modification thereof) should be adequate to reduce heavy flavor backgrounds to a very subdominant level, while keeping the majority of the signal.

We reconstruct jets using the anti-k_T algorithm [62] with $R = 0.4$, keeping those with $p_T > 50$ GeV and $|\eta| < 2.5$. No b-tags are applied. Each lepton is then paired with the hardest jet which satisfies $\Delta\phi(j, \ell) < \pi/2$ and $m(j, \ell) < 200$ GeV.[10] Cases with too few or non-unique pairings are discarded.

Our missing energy reconstruction is very naive, and hopefully conservative: we simply balance the summed $\vec{p}_T$ of the two leptons and the two "b-jets."

We find that reducible backgrounds from $\ell^+\ell^-$+jets (including taus) and W^+W^-+jets are quite small throughout our analysis after all cuts, each at the 1–10% level with respect to the irreducible dileptonic $t\bar{t}$.[11] In what follows, we explicitly keep only the irreducible background, which is by far our biggest concern.

---

[9] We do not include interference effects between the resonance and Standard Model in the ensuing analysis, since we expect them to be largely washed-out when integrating over the peak and taking the absolute value $|\phi_\ell + \bar{\phi}_\ell|$. Nonetheless, we have explicitly checked a small set of realistic, fully interfered samples with 15% resonance width, pure vector couplings to light quarks (to maximize the persistence of the interference given the chirality-averaged initial state), and vector or axial couplings to tops. We find that with $S/B \simeq 1$ in the resonance region, our azimuthal distributions are consistent with an incoherent average of the signal and background.

[10] For genuine boosted top decays, the b-jets are quite narrow, and their directions should be easy to accurately measure using the tracker. We therefore assign no error beyond energy smearing in the reconstruction of the jet-lepton invariant mass, nor in any of our subsequent kinematic reconstructions.

[11] To reduce the former background to this level, we require a simple Z-veto that rejects same-flavor lepton pairs with $m(\ell^+, \ell^-) = [75, 105]$ GeV. This has a very minor effect on our signal, but order-of-magnitude effect on $\ell^+\ell^-$+jets.

B. Reconstruction of $m_{t\bar{t}}$

The most efficient way to separate our signal from the continuum $t\bar{t}$ background is to measure $m_{t\bar{t}}$ and isolate the resonance region. However, since we will investigate spin correlations in the dileptonic channel, we face an inevitable complication due to the two missing neutrinos. Of course, by the time a dileptonic analysis becomes sensitive to the resonance, we should already know the resonance's mass (and perhaps also its width) quite well from measurements in l+jets and all-hadronic modes. So if we can reconstruct $m_{t\bar{t}}$, even approximately, then we already know where to look.

The two neutrinos represent six lost kinematic degrees of freedom, only two of which are recovered through the measurement of $\vec{\not{E}}_T$. Complete kinematic reconstruction is nonetheless possible by demanding on-shell tops and Ws on the two sides of the event, which fix the other remaining four degrees of freedom through four constraints. For energetic top pairs, the possible kinematic ambiguity regarding which b-jet belongs to which lepton is not a major issue, and solving for the complete system essentially reduces to finding the zeros of a quartic polynomial [63]. There are always four complex solutions, of which either zero, two, or four might be real.[12]

This type of direct solution approach is not without its dangers. The continuum $t\bar{t}$ background at the LHC rises steeply toward small $m_{t\bar{t}}$, and even a modest rate of misreconstruction can "avalanche" low-mass backgrounds into our high-mass signal region. Indeed, the full kinematic solution can be highly sensitive to the precise values of visible kinematic variables, as well as to the detailed choice of top and W masses used to find the solutions.[13] The situation is particularly difficult for energetic tops, as all of the decay products, including the neutrinos, approximately fall on a single axis in the transverse plane, and the neutrinos are roughly back-to-back. Accurate event reconstruction then demands exceptionally good measurement of missing energy components.

The alternative is to consider reconstructions which are safer from the perspective of overestimating the mass of backgrounds, but which do so by actively attempting to *underestimate* the true mass. A well-known example (advocated for dileptonic $t\bar{t}$ resonance reconstruction in [65]) is the cluster transverse mass,

$$M_{T\text{cl}}^2 \equiv \left(\sqrt{p_{T\text{vis}}^2 + m_{\text{vis}}^2} + \not{E}_T \right)^2 - \left(\vec{p}_{T\text{vis}} + \vec{\not{E}}_T \right)^2, \tag{23}$$

with the "vis" subscript referring to the 4-vector sum of the two leptons and two b-jets. This represents the smallest $m_{t\bar{t}}$ consistent with the measured $\vec{\not{E}}_T$, without any on-shell

---

[12] A more realistic experimental analysis might instead solve the system using a multivariate likelihood approach (see, e.g., [64]), allowing all of the measured transverse observables ($\vec{\not{E}}_T$, $\vec{p}_T(l_i)$, $\vec{p}_T(j_i)$) to vary, approximately within their errors, along with the unknown neutrino 3-momenta. This always gives real solutions by construction, and multiple solutions can be ranked or weighted by their likelihoods.

[13] Even the natural Breit-Wigner scatter in the true event-by-event top and W masses produces sizable tails in the reconstructed $m_{t\bar{t}}$ at parton-level.

criteria for the tops and Ws.[14] We can also try to improve upon this a bit by utilizing the fact that the neutrinos should be roughly collinear with the visible products when the tops are boosted. To this end, we construct a kind of minimal single neutrino, which under-reconstructs the complete $\nu\bar{\nu}$ subsystem, by setting $\vec{p}_T(\nu) \equiv \vec{\slashed{E}}_T$ and setting η to match that of the closest lepton in ϕ. (Setting η to match the rapidity of the closest $b + l$ system yields nearly equivalent results.) In addition, we could consider the M_{eff} variable used in supersymmetry searches, which simply adds up the scalar p_Ts of all visible products and $\slashed{E}_T$. We could also choose to be even more minimalistic, and just take the invariant mass of the visible component of the event.[15]

To determine a reasonable method for our present work, amongst the many available options, we study a handful of kinematic reconstructions. In addition to the four under-complete reconstructions just described, we also consider two methods based the complete reconstruction using mass constraints, for which we must solve a quartic equation. While the quartic will practically never yield exactly one real solution, and often yields zero real solutions, we find that a simple and conservative workaround is to take the real components of the neutrino momenta returned by the solutions, and pick the configuration that yields the smallest $m_{t\bar{t}}$. We also include the strategy of Bai and Han [52], which discards solutions that give the neutrinos too large a fraction of the scalar p_T of the event, or which have imaginary components that are too large. Complex solutions are then made real by taking the complex norm of the reconstructed top and anti-top 4-momentum components, and all acceptable solutions are included with equal weight. (Complex solutions are only counted once.) Equivalently for our purposes, we just pick one solution at random.

In Figs. 1 and 2, we show the results of our reconstructions on narrow 1 and 2 TeV spin-1 vector-coupled resonances and on the SM continuum at the 14 TeV LHC, including an additional reference reconstruction where the neutrino 3-vectors are perfectly measured.[16,17] Roughly speaking, there is a tradeoff between how tightly we attempt to sculpt the core of the

---

[14] More specifically, this is realized by a kinematic configuration where the neutrinos are exactly collinear in 3D (the precise energy-sharing is irrelevant), are aligned with $\vec{\slashed{E}}_T$ in the transverse plane, and have rapidity matching that of the visible cluster. For generalizations of this method to cases where the missing particles are massive (they should again be set 3D-collinear, but all moving with the same velocity), see [66, 67].

[15] Perhaps the *most* minimalistic strategy, simply applying a hard cut to the p_T of the leptons, was used in [68]. This is fairly inefficient, so we do not pursue it here. However, in cases where the resonance has enough cross section, this may be a clean and effective way to get a reliable signal sample. We note that for highly boosted tops, the lepton p_T is largely uncorrelated with the azimuthal angles about the production axis, and we suspect that our correlation measurements will continue to work even with such a manifestly kinematically-biased cut.

[16] Axial resonances look nearly identical, while purely RH chiral resonances tend to have slightly harder distributions, and purely LH slightly softer.

[17] The reconstruction with perfectly measured neutrinos displays a pronounced low-mass tail, partially due
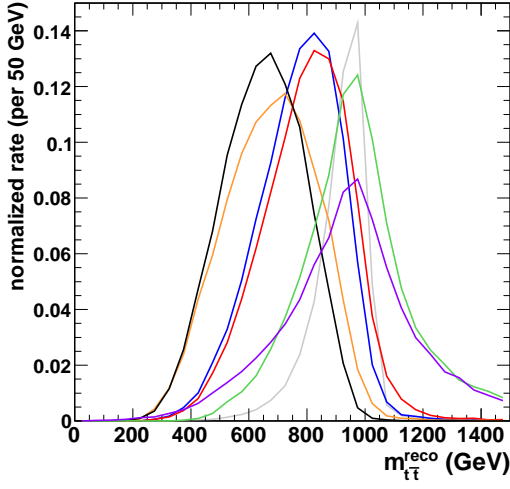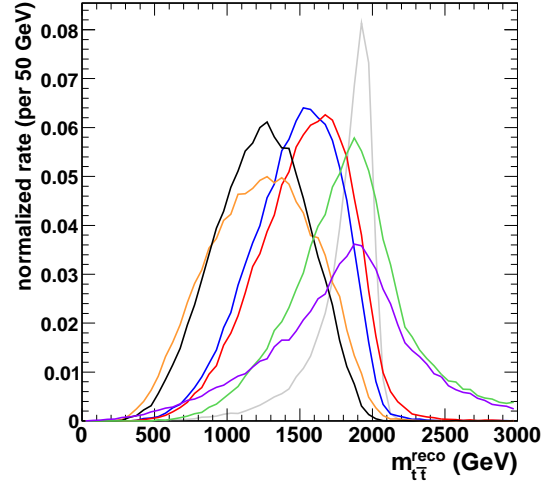
FIG. 1. *Various approximations to $m_{t\bar{t}}$ as applied to narrow 1 and 2 TeV vector resonances. Neutrino reconstructions include perfect (grey, scaled vertically by 1/2), $M_{T\text{cl}}$ (blue), minimal η-collinear (red), visible-only (black), M_{eff} (orange), minimal real-part quartic (green), and Bai-Han quartic (purple).*
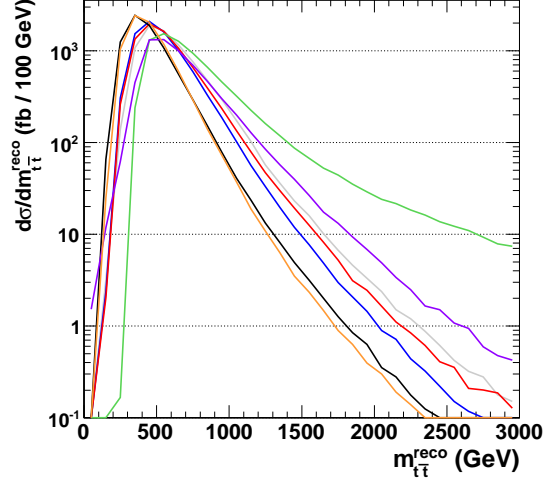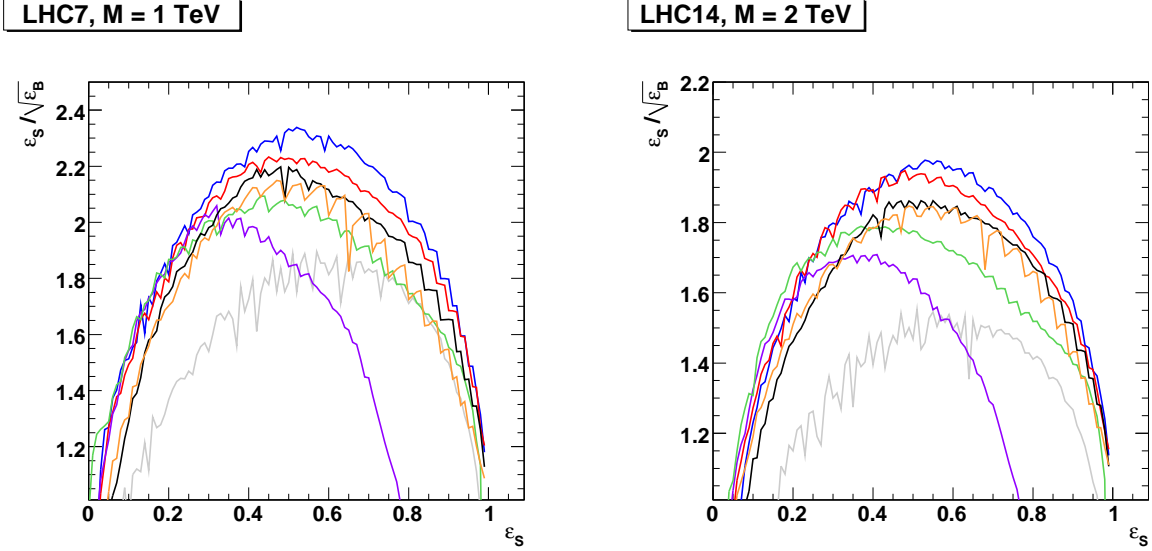

FIG. 2. *Various approximations to $m_{t\bar{t}}$ as applied to continuum Standard Model $t\bar{t}$ at LHC14. Neutrino reconstructions include perfect (grey), $M_{T\text{cl}}$ (blue), minimal η-collinear (red), visible-only (black), M_{eff} (orange), minimal real-part quartic (green), and Bai-Han quartic (purple).*

FIG. 3. *Significance improvement versus signal efficiency, using optimized mass windows and transversity cuts, for a 1 TeV narrow resonance at LHC7, and for a 2 TeV narrow resonance at LHC14. Neutrino reconstructions include perfect (grey, scaled to $(1/2)\varepsilon_S/\sqrt{\varepsilon_B}$), $M_{T\mathrm{cl}}$ (blue), minimal η-collinear (red), visible-only (black), M_{eff} (orange), minimal real-part quartic (green), and Bai-Han quartic (purple). (The 2 TeV curves were generated using a background sample with $m_{t\bar{t}} > 800$ GeV at parton-level, to improve statistics. Therefore the regions near 100% efficiency are not fully accurate. They would have a much steeper slope in reality, and the overall SIC levels on the rest of the plot would be higher. However, even with modest cuts, sensitivity to this generator-level cutoff largely disappears.)*

signal peak and how often we overshoot the true mass. To assess what this means in terms of discriminating signal from background, we run a simple cut optimization study, scanning over possible mass windows. Inspired in part by the observations of [52], we also scan over a cut on the event's "transversity," defined as the ratio of either $M_{T\mathrm{cl}}$, M_{eff}, or $\min(\{p_T(b,l)\})$ to the reconstructed mass. In particular, this type of cut aids in removing a substantial contribution from gluon fusion backgrounds, which tend to peak at low production angles. It also significantly cuts down the unphysical high-mass broadening of the background for the quartic reconstructions.

Some representative results for the narrow resonance optimizations are presented in Fig. 3,

to additional neutrinos lost in semileptonic B-hadron decays, and partially due to FSR of gluons off of the tops. The shape can be improved with the inclusion of extra jets into the reconstruction, though we have erred on the conservative side and not done so.

LHC 7	Mass/Transversity Cuts	$\varepsilon_S^{\text{selection}}$	$\varepsilon_S^{\text{selection+cuts}}$	σ_B
1 TeV, Narrow	$M_{T\text{cl}} = [750, 1025]$ GeV, $M_{\text{eff}}/M_{T\text{cl}} > 0.65$	0.38	0.24	21 fb
1 TeV, 15%-Width	$M_{T\text{cl}} = [700, 1450]$ GeV, $M_{\text{eff}}/M_{T\text{cl}} > 0.65$	0.33	0.19	24 fb
2 TeV, Narrow	$M_{T\text{cl}} = [1600, 2100]$ GeV, $M_{\text{eff}}/M_{T\text{cl}} > 0.50$	0.58	0.20	0.07 fb
2 TeV, 15%-Width	$M_{T\text{cl}} = [1425, 2925]$ GeV, $M_{\text{eff}}/M_{T\text{cl}} > 0.75$	0.40	0.09	0.17 fb

TABLE I. *Optimized mass window and transversity cuts, and the corresponding signal efficiencies and background cross sections, for the 7 TeV LHC. Signal efficiencies are for a vector-like spin-1 resonance in the dileptonic mode, after basic selection and then after application of the cuts.*

LHC14	Mass/Transversity Cuts	$\varepsilon_S^{\text{selection}}$	$\varepsilon_S^{\text{selection+cuts}}$	σ_B
1 TeV, Narrow	$M_{T\text{cl}} = [725, 1000]$ GeV, $M_{\text{eff}}/M_{T\text{cl}} > 0.75$	0.35	0.19	179 fb
1 TeV, 15%-Width	$M_{T\text{cl}} = [700, 1300]$ GeV, $M_{\text{eff}}/M_{T\text{cl}} > 0.75$	0.32	0.16	253 fb
2 TeV, Narrow	$M_{T\text{cl}} = [1475, 2050]$ GeV, $M_{\text{eff}}/M_{T\text{cl}} > 0.60$	0.56	0.27	5.6 fb
2 TeV, 15%-Width	$M_{T\text{cl}} = [1425, 2425]$ GeV, $M_{\text{eff}}/M_{T\text{cl}} > 0.60$	0.48	0.19	7.5 fb

TABLE II. *Optimized mass window and transversity cuts, and the corresponding signal efficiencies and background cross sections, for the 14 TeV LHC. Signal efficiencies are for a vector-like spin-1 resonance in the dileptonic mode, after basic selection and then after application of the cuts.*

using the SIC ("significance improvement characteristic," i.e. $\varepsilon_S/\sqrt{\varepsilon_B}$) visualization of [48]. In practice, we find that M_{eff} usually works best for the transversity cut, and we use it for all of our displayed SIC curves except for that of M_{eff} itself, for which we use $\min(\{p_T(b, l)\})$. We find that the consistently most powerful mass estimator is $M_{T\text{cl}}$, in combination with the cut on $M_{\text{eff}}/M_{T\text{cl}}$. We therefore use these to define the signal regions for our subsequent azimuthal angle analysis, maximizing $\varepsilon_S/\sqrt{\varepsilon_B}$. Tables I and II contain the results of the optimization.

Of course, any conclusions drawn from such a simple study can only be taken as suggestive, but it does indicate that attempts to make detailed reconstructions of the neutrinos might be counterproductive, unless cleverer techniques are brought to bear.[18] It is also not clear that the maximum $\varepsilon_S/\sqrt{\varepsilon_B}$ point is truly the best to maximize the significance of an angular correlation measurement. We make this choice merely for want of a better guide, and, in particular, lack of reliable information about possible systematic errors.

---

[18] We emphasize that the underperformance of the full quartic solutions with respect to $M_{T\text{cl}}$ in this study is not just an artifact of our somewhat pessimistic missing energy reconstruction. The conclusion remains unchanged if we switch to perfect $\vec{\rlap{/}E}_T$ measurement and turn off energy smearings.

C. Measurement of azimuthal observables

In the previous subsection, we investigated six different methods for reconstructing the complete dileptonic $t\bar{t}$ system. Here, we will now determine to what extent these methods can be used to extract azimuthal correlations.

One issue which we must address at this point is how to define the production plane in the reconstructed $t\bar{t}$ CM frame, given that the beams are typically not exactly back-to-back in this frame. A common tactic is to follow the Collins-Soper construction [69], which defines an effective beam axis by taking the difference between the two unit vectors pointing along the beams. We take a slightly simpler route, which we find leads to some improvements in the amplitudes of our azimuthal modulations. We simply bring the $t\bar{t}$system to rest in lab coordinates via a rotation-free boost, and then use the lab's native beam axis for the construction of the production plane.

In Figs. 4 through 6, we show the reconstructed distributions of $(\phi_\ell - \bar{\phi}_\ell)$ and $|\phi_\ell + \bar{\phi}_\ell|$ for a variety of narrow gg-initiated spin-0 resonances and $q\bar{q}$-initiated spin-1 resonances, and for the SM continuum at the 14 TeV LHC. We apply our narrow resonance cuts from Table II to our resonance samples, and broad cuts to the SM samples (which slightly improves statistics). The reconstructions are the same as those discussed in the previous subsection, though we now omit M_{eff}, which does not offer a fully 3D picture of the event. The figures exhibit all of the expected behavior discussed in Section II, for all of the reconstruction techniques.[19] Some are clearly better than others, but interestingly the differences are usually not very dramatic. The clear exception is the minimal real-part quartic solution, which tends to introduce spurious modulations in $(\phi_\ell - \bar{\phi}_\ell)$. However, the remaining reconstructions are all quite good. In particular, we preserve nearly the entire modulation using only *visible* particles (the two leptons and two b-jets).[20] We take this as a strong hint that these angles may be very straightforward to reconstruct in reality, at least in the case of somewhat fast-

---

[19] We do acquire some small $|\phi_\ell + \bar{\phi}_\ell|$ modulations for the scalars and $(\phi_\ell - \bar{\phi}_\ell)$ modulations for the vectors, up to the 10% scale for 1 TeV resonances. These are mainly due to some biases incurred by our selection cuts and jet-lepton pairing strategy, rather than genuine helicity interference. Nonetheless, the effects of these biases also show some correlations with the resonance couplings.

[20] The visible-only ϕ_ℓ's are actually very closely related to angular variables which can be constructed in the top frame, and which are associated with a well-defined analyzing power of about 80%: instead of directly measuring the lepton direction, first boost the $b + l$ composite system to rest (without rotation), and then measure the lepton direction. In our visible construction, we instead immediately boost the $b + l$ system into lab-frame without first bringing it to rest in top-frame, but the resulting ϕ_ℓ is nearly the same. It is even possible to accurately approximate this using purely geometric constructions in the lab
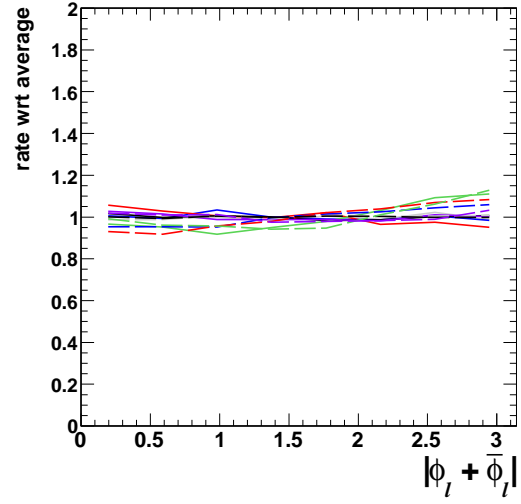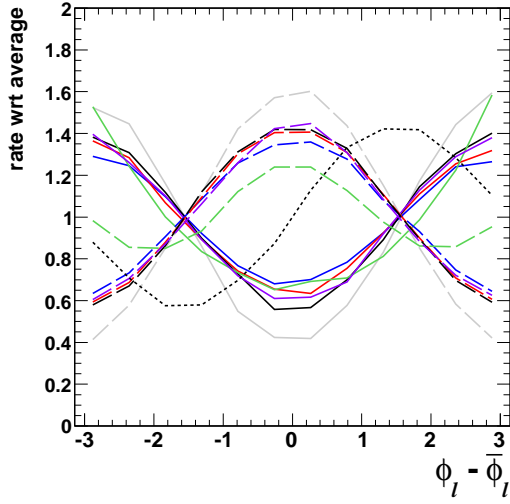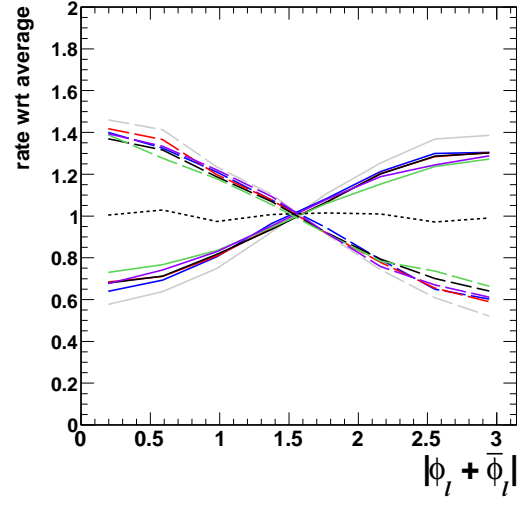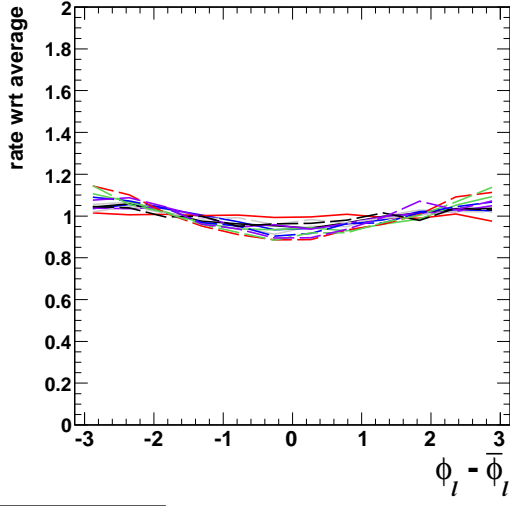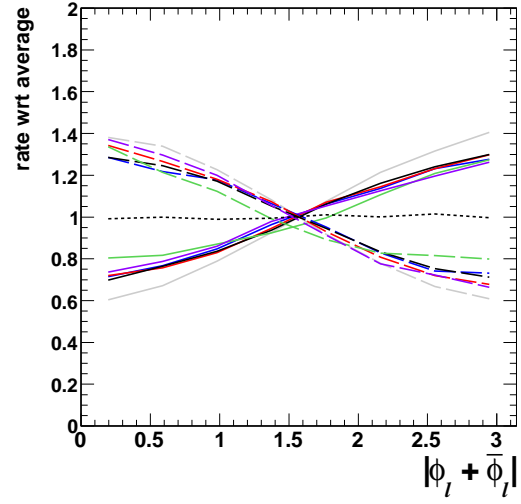
1 TeV Spin-0
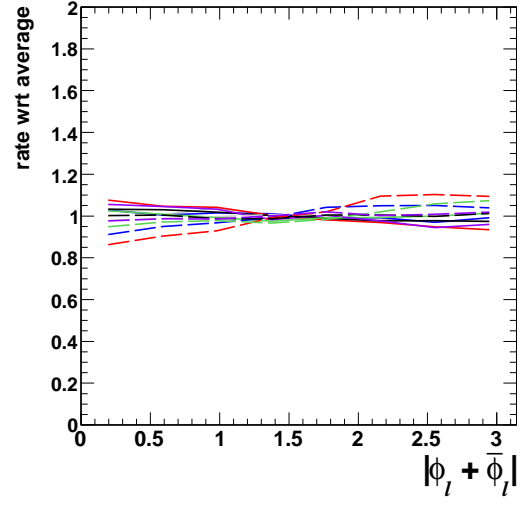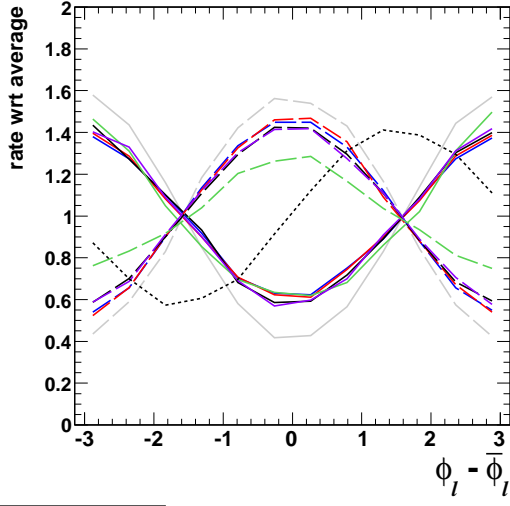
2 TeV Spin-0

FIG. 4. *Distributions of $(\phi_\ell - \bar\phi_\ell)$ and $|\phi_\ell + \bar\phi_\ell|$ for 1 and 2 TeV spin-0 resonances: pure scalar (solid), pseudoscalar (long-dashed), and mixed $\alpha = \pi/4$ (short-dashed). Neutrino reconstructions include perfect (grey), $M_{T\mathrm{cl}}$ (blue), minimal η-collinear (red), visible-only (black), minimal real-part quartic (green), and Bai-Han quartic (purple).*

frame. For example, each of the b-jets can be taken to define an independent z-axis and production plane, with ϕ_ℓ's measured with respect to these coordinate systems. We thank Stephen Parke for suggesting the possibility of using lab-frame angles.
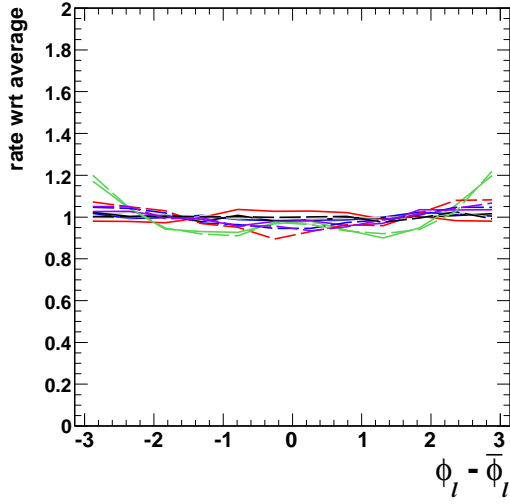
1 TeV Spin-1

2 TeV Spin-1

FIG. 5. *Distributions of* $(\phi_\ell - \bar{\phi}_\ell)$ *and* $|\phi_\ell + \bar{\phi}_\ell|$ *for 1 and 2 TeV spin-1 resonances: pure vector (solid), axial-vector (long-dashed), and left-chirality (short-dashed). Neutrino reconstructions include perfect (grey),* $M_{T\mathrm{cl}}$ *(blue), minimal* η*-collinear (red), visible-only (black), minimal real-part quartic (green), and Bai-Han quartic (purple).*

moving tops where the visible products can be cleanly separated into hemispheres. The fact that the semileptonic top decay is roughly 2/3 visible is clearly a tremendous help here, as the vector-sum of its visible activity gives us an adequate approximation of the true top direction of flight. Moreover, our cuts bias us away from kinematic configurations where the neutrinos are dominating.
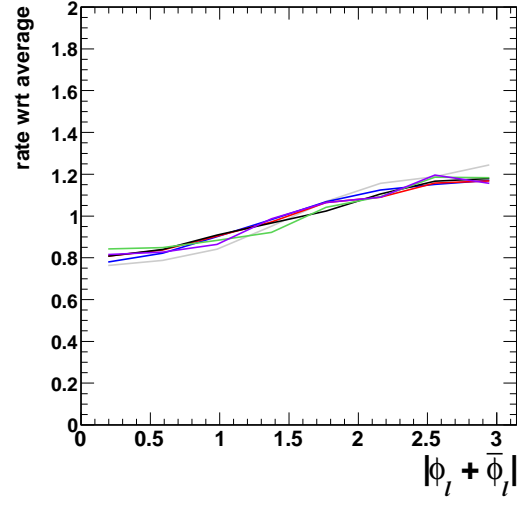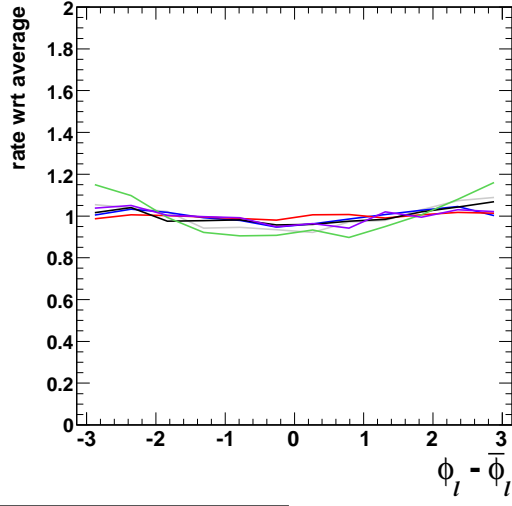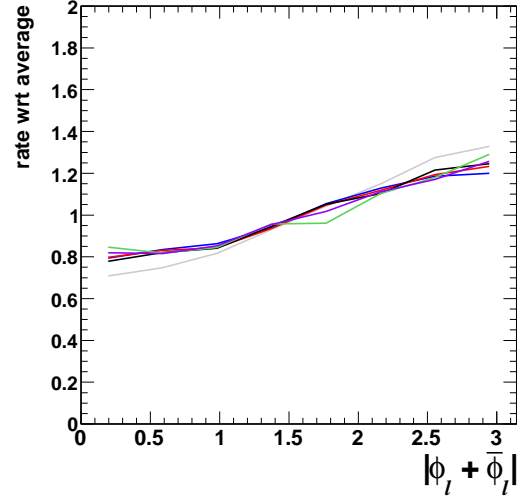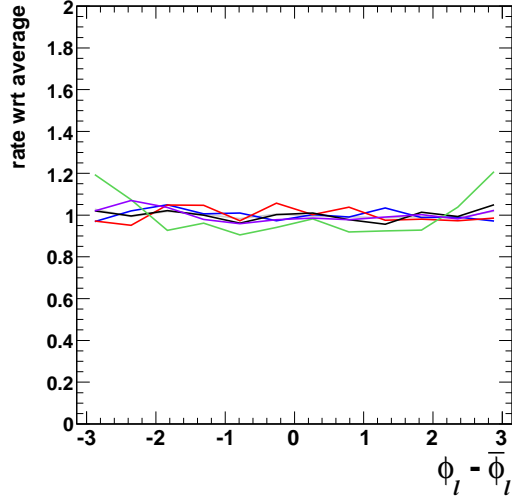
FIG. 6. *Distributions of* $(\phi_\ell - \bar{\phi}_\ell)$ *and* $|\phi_\ell + \bar{\phi}_\ell|$ *for Standard Model* $t\bar{t}$ *at LHC14 in 1 and 2 TeV (broad) mass windows. Neutrino reconstructions include perfect (grey),* $M_{T\mathrm{cl}}$ *(blue), minimal* η-collinear neutrino (red), *visible-only (black), minimal real-part quartic (green), and Bai-Han quartic (purple).*

A detailed understanding of the observability of these modulations in the presence of background and systematic uncertainties is beyond the scope of this paper. However, we can make some rough estimates for the timely question of discriminating a true vector from an axial-vector. For this purpose, we can think of the $|\phi_\ell + \bar{\phi}_\ell|$ distribution with only two bins, i.e. as an asymmetry of roughly $\pm 25\%$. From a purely statistical perspective,

with no background, these two cases could be discriminated at 3σ level if the error on the asymmetry can be brought down to the 15% level. This would require less than 100 events. Given that, after cuts, we accept only about 20% of the dileptonic signal, and hence 1% of the total $t\bar{t}$ resonance signal, this kind of analysis becomes statistically possible when the LHC accumulates $O(10,000)$ $t\bar{t}$ pairs from the resonance. We would therefore require cross sections at the pb-scale for the LHC7 (assuming 5–10 fb^{-1}), and at the 100 fb-scale for the long-term LHC14. Interestingly, for ℓ+jets, which has six times higher branching fraction but 40% as much modulation (if we correlate with the b-quark on the hadronic side), the required cross sections would naively not be so different. On the other hand, different factors come into play, in particular the need to identify b-(sub)jets and to possibly run a hadronic top-tagger (as in, e.g., [60, 70–76], and reviewed in [77]), but also presumably larger efficiency and better resonance peak reconstruction.

Of course, if $S/B \lesssim 1$, the discrimination becomes more challenging. Besides diluting the signal, the Standard Model continuum also exhibits its own vector-like $(\phi_\ell + \bar{\phi}_\ell)$ modulation. Accurate extraction of the signal modulation would therefore require a well-controlled background subtraction. Assuming this can be done, then models with $S/B \simeq 1$ could probably be discriminated at 3σ with at least a few hundred dileptonic signal and background events after cuts. From Table I, we see that the SM backgrounds to a 1(2) TeV analysis after 10 fb^{-1} at the LHC7 would be roughly 200(1) events. We are background-limited only for resonances at or slightly above 1 TeV, requiring multi-pb cross sections. Heavier resonances are rate limited. For 100 fb^{-1} at LHC14, even 2 TeV resonances will be background-limited, requiring low pb-scale for the signal. While we have not investigated even higher resonance masses, these again quickly become rate-limited at the 14 TeV machine, with 100 fb yielding adequate statistics to discriminate vector from axial-vector in the dileptonic mode.

Given these estimates, what might we expect to learn about axigluon-like models applicable to the Tevatron top A_{FB} anomaly? The size of the asymmetry (central value near 50% for $m_{t\bar{t}} > 450$ GeV [1]) and the lack of major deviations from the SM prediction for $d\sigma/dm_{t\bar{t}}$ [78, 79] favor a heavy resonance with large couplings. At the same time, LHC searches for dijet resonances and contact interactions [80, 81] constrain the couplings to quarks. While we do not undertake a full scan of the parameter space, we can use the analysis of [10] to identify a reasonable example of a phenomenological model, consistent at 68% CL with the Tevatron anomaly and having modest impact on $d\sigma/dm_{t\bar{t}}$: a 1.5 TeV resonance with purely axial couplings to light quarks and top quarks of $g_A^q = (0.7)g_s$ and $g_A^t = (-3.0)g_s$.[21] Assuming that b_L also couples with the same strength as the tops, the width is about 18%, and the branching fraction to tops is close to 57% (to light quarks it is about 14%). This resonance easily evades the exclusion limits on universal axigluons and on

---

[21] The contribution to A_{FB} in the $m_{t\bar{t}} > 450$ GeV bin would be about 27% at parton-level. Combined with the NLO contribution from the Standard Model, this brings the asymmetry to within 1σ of the measured value.

more general dijet resonances in the recent ATLAS search [80], is safe from quark contact interaction constraints,[22] and is below the current CMS limit on top resonances [82]. At LHC7, $\sigma \times BR(t\bar{t})$ is about 4 pb, and the optimal M_{Tcl} window should be highly signal dominated. A 5–10 fb^{-1} data set should therefore be enough to establish a pure axial interpretation over a pure vector interpretation to at least 3σ for this model. Clearly, then, azimuthal decay correlations could potentially have a nontrivial part to play in disentangling the full story behind the Tevatron A_{FB} anomaly, even for the early phase LHC.

It is also worth noting that our analysis could still apply to cases without a well-defined resonance peak. For axigluon-like resonances well above 1 TeV, matching the size of the Tevatron anomaly requires large couplings, and therefore typically quite large width ($\Gamma/M \gtrsim 20\%$). This may simply show up as a broad excess over the Standard Model at high mass. However, neglecting for the moment interference with the Standard Model, none of our results were actually sensitive to *where* we looked on the resonance's Breit-Wigner curve. Indeed, while a broad resonance signal may be difficult to isolate on-peak, it can come to dominate the high-mass tail of $t\bar{t}$ production. With a full 14 TeV LHC at $O(100)$ fb^{-1} luminosity, this tail will be very well-populated by the Standard Model alone. For example, the region above 2 TeV should contain $O(10,000)$ central QCD-induced events, and this number may be substantially enhanced by the resonance.

Still, the final fate of such an analysis becomes more model-dependent, as interference with the Standard Model could be non-negligible. This affects not only the total rate, but also the coefficient of $\cos(\phi_\ell + \bar{\phi}_\ell)$, in proportion to the product of the light quark and top quark vector charges. Notably, this interference is washed-out if either the top quarks or the light quarks are mostly axially coupled. See Appendix B for a more detailed discussion.

IV. CONCLUSIONS

The discovery of a resonance in the $t\bar{t}$ invariant mass spectrum at the LHC would represent the beginning of a major advance in our understanding of TeV-scale physics. In the event of such a discovery, determining the precise nature of this resonance will become one of the highest priorities of the LHC experimental program. Fortunately, the very distinctive decays of top quarks will give us the opportunity to address rather detailed questions about the resonance's couplings. Unlike the case of a resonance decaying directly into stable particles such as electrons, different $t\bar{t}$ helicity channels coherently interfere as they decay into the same set of 6-body final-states. The final decay distributions, correlated between top and antitop, therefore carry information about signs/phases in the tops' chiral production matrix elements.

---

[22] We have explicitly checked that the contribution to central dijet production in each of ATLAS's mass bins, including full interference and t-channel exchanges, is below the stated uncertainties.

We have argued in this paper that the tops' azimuthal decay distributions about their production axis provide a sensitive and experimentally robust probe of these correlations. As is usual for $t\bar{t}$ spin correlations, the charged lepton (or down-type quark) exhibits the largest effects. Spin-0 resonances lead to 60% modulations in $(\phi_\ell - \bar{\phi}_\ell)$, with a phase offset that directly represents the resonance's CP phase. Spin-1 and spin-2 resonances lead to modulations in $(\phi_\ell + \bar{\phi}_\ell)$, with a signed magnitude that depends on the ratio of chiral couplings, $(30\%) \times 2 \,/\, (g_L/g_R + g_R/g_L)$ when integrated over production angles (two times larger when restricting to highly central production). While the spin-0 CP phase has long been a topic of investigation, the spin-1(2) chiral coupling ratio is largely missed in common top spin correlation variables such as the double-cosine distribution and the 3D lepton opening angle. We have found that single-differential azimuthal sum/difference distributions contain all of the relevant information contained in these more common variables, and more.

We have also found that these azimuthal distributions are straightforward to reconstruct, without detailed information on neutrino kinematics. We established this point in the dileptonic mode, in which variables sensitive to spin correlations usually require complicated reconstruction techniques. In contrast, azimuthal distributions can be well-approximated using only visible kinematics. The major nontrivial task then becomes isolating the resonance region by reconstructing $m_{t\bar{t}}$. Our own (admittedly limited) investigation suggests that simple reconstructions such as $M_{T\mathrm{cl}}$ may be superior to more complete reconstructions that utilize on-shellness criteria on the Ws and tops. However, this conclusion could still change in a more detailed experimental study, or with better reconstruction techniques.

Since the modulations are large in the dileptonic mode, measuring them should not require a very big event sample. For example, $O(100)$ events should be adequate to discriminate a pure vector resonance from an axial-vector resonance at better than 3σ level, assuming $S/B \gtrsim 1$. For favorable choices of parameters, a color-octet axial-vector resonance could explain the Tevatron A_{FB} anomaly, be discovered at the early LHC, *and* have its mostly-axial coupling to tops confirmed not long afterwards. This would be a dramatic interplay between the capabilities of the two colliders.

While we have focused on dileptonic $t\bar{t}$, the option of using the ℓ+jets mode will also be important to explore in more detail. Extracting the smaller modulations may require greater control over systematics, but the much higher statistics and much better kinematic reconstruction afforded by this channel could easily offset this. In particular, for resonances well above 2 TeV, ℓ+jets may be the only viable option, even for the long-term LHC, due to the smaller cross sections involved.

We have also limited ourselves to simulations based on leading-order $t\bar{t}$ production and decay, with additional radiation and kinematic rearrangements provided by the `PYTHIA` virtuality-ordered parton shower. Understanding the genuine NLO behavior of the azimuthal correlations, processed through realistic event reconstructions, remains as an interesting open task which can potentially be addressed by modern calculations [83–85].

Finally, while the focus of this work has been characterization of physics beyond the Standard Model, we note that azimuthal decay angles could also be useful for detecting the spin correlations of boosted or semi-boosted tops from pure QCD (*cf.* the modulations in Fig. 6), and serve as a particularly clean indication that the top quark is spin-1/2.

Appendix A: Basic Definitions and Spin-0

In Section II, we gave various formulas for $d\Gamma$ over different portions of the angular phase space, including the production angle of the $t\bar{t}$ pair in the $t\bar{t}$ CM frame and the decay angles for the two leptons. In these appendices, we present these formulas in a more complete form, displaying all angular correlations. We also go beyond the chiral $m_t = 0$ limit. Though this is likely to be a reasonable approximation for resonances at 1 TeV or higher, finite-mass effects are not always totally negligible. We parametrize them with factors of $r \equiv 2m_t/M$ (the inverse Lorentz boost of the tops) and $\sqrt{1 - r^2}$ (the tops' velocities). However, we continue to ignore velocity-suppression factors that arise purely from $t\bar{t}$ phase space, which in any case can be factorized out of the total resonance decay rate. We also neglect interference terms with the SM. These effects tend to be small on-peak. There are, of course, cases where the interference is nonetheless more important than the finite-mass corrections. We outline out the effects of interference in more detail below.

Recalling Section II, we define our coordinate system as follows. We first find the $t\bar{t}$ production axis in the $t\bar{t}$ CM frame. The angle that this makes with the beam axis is called Θ, and we average over configurations $\Theta \leftrightarrow \pi - \Theta$. We then perform rotation-free boosts to bring both tops to rest. We define a common z-axis using the original t direction. To define the y-axis, we take either of the two unit vectors perpendicular to $t\bar{t}$ production plane, and then define the x-axis to make a right-handed 3D coordinate system.

Before proceeding, we note that all of the equations that we give can apply to arbitrary pairs of top decay products. For example, in the ℓ+jets channel we might correlate the lepton with the b-jet from the hadronic side. Starting with the full angular distributions for two leptons, upon changing to the angular variables for the particles of interest, we need

only multiply each sin and cos of the new polar angle by the appropriate spin-analyzing power: 1 for leptons, -0.3 for neutrinos, -0.4 (+0.4) for b-quarks (W-bosons), and 0.5 for the softer of the two W decay products in the top rest frame.[23,24] We subsequently drop the "ℓ" subscript from all of the angular variables, as an implicit reminder that we are no longer restricted to dileptonic mode.

The angular formulas for spin-0 decay were given in Section II A to zeroth order in r. Restoring the full kinematic dependence, we get

$$\frac{d^4\Gamma}{d\Omega \, d\bar{\Omega}} \propto 1 + \cos\theta \cos\bar{\theta} - \sin\theta \sin\bar{\theta}\Big(\cos(2\alpha)\cos\big(\phi - \bar{\phi}\big)$$

$$-\sqrt{1-r^2}\sin(2\alpha)\sin(\phi - \bar{\phi})\Big)$$

$$-\frac{1}{2}r^2\big(1 + \cos(2\alpha)\big)\big(1 + \cos\theta\cos\bar{\theta} - \sin\theta\sin\bar{\theta}\cos(\phi - \bar{\phi})\big),$$

$$\frac{d\Gamma}{d(\phi - \bar{\phi})} \propto \Big(1 - r^2\cos^2\alpha\Big)$$

$$-\Big(\frac{\pi}{4}\Big)^2\Big(\big[\cos(2\alpha) - r^2\cos^2\alpha\big]\cos(\phi - \bar{\phi}) - \sqrt{1-r^2}\sin(2\alpha)\sin(\phi - \bar{\phi})\Big), \text{(A1)}$$

where 2α is the relative phase between the $\bar{t}_L t_R$ and $\bar{t}_R t_L$ couplings. Values of α besides 0 and $\pi/2$ signify CP violation. The upper formula is the "master" leptonic angular distribution from which one can derive the dependence on whatever angular variable one wishes. The lower equation describes the azimuthal correlations, which we found useful for identifying a heavy particle's relative couplings to different top chiralities regardless of its spin. In this case, the dependence is in $(\phi - \bar{\phi})$. For spin-0, $(\phi + \bar{\phi})$ is a physically meaningless quantity, though we will see below that spins 1 and 2 have their leading modulations in it. Formulas for the traditional distributions in $\cos\theta\cos\bar{\theta}$ and $\cos\chi$ are given in Section II.

In addition to the finite-boost corrections, we can also consider the effects of interference with the Standard Model. First, we note that these effects vanish for a scalar produced in $q\bar{q}$ annihilation, since to very good approximation the QCD contribution only takes place between quarks of opposite helicity (same spin). For gg fusion, the interference vanishes at high boost, as the QCD contribution dominantly proceeds from same-spin gluons to same-spin (chiral) tops. The interference is also suppressed relative to the "resonance-squared" contribution since the interference term crosses a zero on-peak. Integrating the interference contribution across the peak (accounting for imperfect cancellation due to falling PDFs and/or asymmetric signal window), the total relative suppression goes as $r(\Gamma/M)^2$. In the case of a color-singlet scalar with generic couplings to $G^{a\mu\nu}G^a_{\mu\nu}$ and $G^{a\mu\nu}\tilde{G}^a_{\mu\nu}$, the

---

[23] Note that care should be taken if, for example, we decide instead to define the z-axis by following the direction of the semileptonic top in ℓ+jets. In that case, the formulas for the ℓ^++jets events stay the same, but for the ℓ^-+jets events they require replacements $\theta \to \pi - \theta$ and $\bar{\theta} \to \pi - \bar{\theta}$.

[24] The analyzing powers for particles other than the lepton are only formally correct under the assumption that the phase space of the remaining particles is fully integrated. In principle, they could change after accounting for detector acceptance and analysis cuts.

interference in the $(\phi - \bar{\phi})$ modulation is controlled by the latter coupling for production nearly perpendicular to the beamline (and swamped by the quasi-singular pure QCD rate for production near the beamline). While the resonance-squared contribution exhibits a modulation $\cos(\phi - \bar{\phi} + 2\alpha)$, the interference comes in with $\sin(\phi - \bar{\phi} + \alpha)$, for example signalling CP-violation when the resonance couples to tops as a pure scalar $(\alpha = 0)$ and to gluons as a pure pseudoscalar. For a 1 TeV resonance of 20% width, we estimate that the size of the interference contribution relative to the resonance-squared is less than 20% if $S/B > 1/4$. This relative contribution decreases with increasing mass, decreasing Γ/M, or increasing S/B.[25]

Appendix B: Spin-1

We give the tops' coupling to a spin-1 particle in Eq. 11. Since the interactions involve same-chirality fields, the left- and right-handed couplings are independent in the absence of parity. We parametrize the different chiral couplings as follows,

$$g_L = g \cos \xi$$
$$g_R = g \sin \xi. \tag{B1}$$

Just as with the scalar case, including $m_t \neq 0$ in the resonance decay will modify the differential decay rate. Since the equivalence of chirality and helicity breaks down with finite fermion mass, all possible spin pairings contribute, though only $\uparrow\uparrow$ and $\downarrow\downarrow$ remain in the limit $r \to 0$.

As mentioned above, producing a spin-1 resonance with zero angular momentum along the beam axis requires gluon fusion, which only occurs via a higher-dimension operator. We therefore begin with formulas for the likely more dominant scenario of $J_{\text{beam}} = \pm 1$ via $q\bar{q}$ annihilation.

Including the dependence on the production angle and all decay angles (choosing one particle each from the t side and $\bar{t}$ side), we get

$$
\begin{aligned}
\frac{d^5 \Gamma_{J_{\text{beam}} = \pm 1}}{d\Omega \, d\bar{\Omega} \, d\cos\Theta} \propto{}& \left(1 + \cos^2\Theta\right)\left(1 - \cos\theta\cos\bar{\theta} + \sqrt{1 - r^2}\cos(2\xi)\left(\cos\bar{\theta} - \cos\theta\right)\right) \\
& - \sin(2\xi)\sin^2\Theta\sin\theta\sin\bar{\theta}\cos(\phi + \bar{\phi}) \\
& + \frac{1}{2}r\Big[\left(1 + \sin(2\xi)\right)\sin(2\Theta)\left(\cos\theta\sin\bar{\theta}\cos\bar{\phi} + \cos\bar{\theta}\sin\theta\cos\phi\right) \\
& \qquad + \sqrt{1 - r^2}\cos(2\xi)\sin(2\Theta)\left(\sin\theta\cos\phi - \sin\bar{\theta}\cos\bar{\phi}\right)\Big] \\
& - r^2\Big[\cos^2\Theta - \sin(2\xi) + \left(\sin(2\xi)\cos^2\Theta - 1\right)\cos\theta\cos\bar{\theta}
\end{aligned}
$$

---

[25] Quite generally, we can infer that the relative contribution of interference within a mass window of width $O(\Gamma)$ centered on the resonance is at most $(\Gamma/M)/\sqrt{S/B}$, with a typically $O(1)$ coefficient that depends on the specific process. In our case, this coefficient carries an additional suppression factor of r.

$$+ \sin^2 \Theta \sin \theta \sin \bar{\theta} \left(\cos \phi \cos \bar{\phi} + \sin(2\xi) \sin \phi \sin \bar{\phi} \right) \Big]. \qquad \text{(B2)}$$

From this distribution, we can integrate and/or change variables to get a function of whatever angular variables we want. We start by demonstrating the claim made in Section II that for a sufficiently light resonance, one can determine the extent to which it is vector or axial with the traditional $\cos \theta \cos \bar{\theta}$ distribution. We can see the difference by setting $\xi = \pi/4$ or $3\pi/4$ and integrating the other angles in Eq. B2. Dividing out by a common numerical prefactor, we get

$$\frac{d\Gamma_V}{d \cos \theta \, d \cos \bar{\theta}} \propto \left(1 + \frac{r^2}{2} \right) - \left(1 - \frac{r^2}{2} \right) \cos \theta \cos \bar{\theta}$$

$$\frac{d\Gamma_A}{d \cos \theta \, d \cos \bar{\theta}} \propto (1 - r^2)\left(1 - \cos \theta \cos \bar{\theta} \right). \qquad \text{(B3)}$$

Firstly, we note that this reproduces the values listed in Table II of Ref. [23]. We see that the ratio of modulating to constant term for the vector only approaches that of an axial resonance in the chiral limit. This difference at nonzero r allows one to separate the two cases, though for M above 1 TeV, this requires fitting the 2D distribution to percent-scale precision. Lastly, we note that the decay amplitude vanishes for an axial-vector at $t\bar{t}$ threshold. This is simple to understand with parity. An axial vector is even under P, while the exchange of $t\bar{t}$ in the final state is odd. For the fermion pair at rest, there is no orbital contribution to the wavefunction that can make up the difference, so the amplitude shuts off. We give the distributions in $(\phi + \bar{\phi})$, $(\phi - \bar{\phi})$ in Eq.B5.

For completeness, we include the analogue of Eq. B2 for $J_{\text{beam}} = 0$, as would arise for a color-octet produced in gluon fusion. Production of such a state is usually suppressed due to the need for higher-dimension interactions, but could dominate if dimension-four couplings to light quarks are small. The 5D distribution in leptonic and production angles is

$$\frac{d^5 \Gamma_{J_{\text{beam}}=0}}{d\Omega \, d\bar{\Omega} \, d\cos \Theta} \propto \sin^2 \Theta \Big(1 - \cos \theta \cos \bar{\theta} + \sin(2\xi) \sin \theta \sin \bar{\theta} \cos(\phi + \bar{\phi})$$

$$+ \frac{1}{4} \sqrt{1 - r^2} \cos(2\xi) \left(\cos \bar{\theta} - \cos \theta \right) \Big)$$

$$- \frac{1}{8} r \Big[\left(1 + \sin(2\xi) \right) \sin(2\Theta) \left(\cos \theta \sin \bar{\theta} \cos \bar{\phi} + \cos \bar{\theta} \sin \theta \cos \phi \right)$$

$$- \sqrt{1 - r^2} \cos(2\xi) \left(\sin \bar{\theta} \cos \bar{\phi} - \sin \theta \cos \phi \right) \Big]$$

$$+ \frac{1}{2} r^2 \Big[\left(1 + \cos(2\Theta) \sin(2\xi) \right) \left(\cos \theta \cos \bar{\theta} - \sin \theta \sin \bar{\theta} \sin \phi \sin \bar{\phi} \right)$$

$$+ \left(\cos(2\Theta) + \sin(2\xi) \right) \left(1 - \sin \theta \sin \bar{\theta} \cos \phi \cos \bar{\phi} \right) \Big]. \qquad \text{(B4)}$$

From Eqs. B2 and B4, we derive azimuthal distributions for polarizations ± 1 and 0,

$$\frac{d\Gamma_{J_{\text{beam}}=P}}{d(\phi + \bar{\phi})} \propto \left(1 + \frac{1}{4} r^2 \left(3 \sin(2\xi) - 1 \right) \right) - \zeta_P \left(\frac{\pi}{4} \right)^2 \left(\sin(2\xi) + \frac{1}{2} r^2 \left(1 - \sin(2\xi) \right) \right) \cos(\phi + \bar{\phi})$$

$$\frac{d\Gamma_{J_{\text{beam}}=P}}{d(\phi-\bar{\phi})} \propto \left(1 + \frac{1}{4}r^2\big(3\sin(2\xi)-1\big)\right) - \frac{1}{4}r^2\left(\frac{\pi}{4}\right)^2\big(1+\sin(2\xi)\big)\cos(\phi-\bar{\phi}), \qquad \text{(B5)}$$

where $\zeta_P = (1/2, -1)$ for $P = (\pm 1, 0)$, respectively. It is straightforward to see why the different polarizations have the same $(\phi-\bar{\phi})$ dependence. The $(\phi-\bar{\phi})$ modulation arises from mass-suppressed "wrong-helicity" ($\uparrow\downarrow$ or $\downarrow\uparrow$) $t\bar{t}$ production. Once Θ is integrated out, this spinless configuration of tops cannot display any residual dependence on the resonance polarization.

Our discussion thus far has focused on the resonance-squared contribution to the total rate, but there is also interference with SM $t\bar{t}$ production. This is a small effect on-peak for narrow resonances, and even for broad resonances if the couplings are large compared to QCD. Still, in a full analysis, one should account for such effects, especially as they may be numerically important relative to the subleading r^2 corrections in $e.g.$ Eq. B5. Let us consider in detail the case of $q\bar{q}$ annihilation into a spin-1 resonance. The interference comes out proportional to the light quarks' vector charges (having averaged over forward and backward directions as well as incoming quark chiralities), and consists of two terms. One is a $\cos(\phi+\bar{\phi})$ modulation, which simply tracks the total cross section interference with the SM, and is proportional to the top's vector coupling. This passes through a zero on-peak, as the resonance propagator goes 90-degrees out of phase with the gluon propagator. Thus, we get a sizable interference effect on-peak only if the light quark and top quark charges each have relatively large vector components, and if the off-peak contributions in our resonance mass window are highly imbalanced. The second interference term is proportional to the top axial charge, and introduces a $\sin(\phi+\bar{\phi})$ contribution to the modulation. This term is suppressed by Γ/M, and would have been averaged out in our analysis of Section III C, which only looked at $|\phi+\bar{\phi}|$. (Note that a sinusoidal modulation component in $(\phi+\bar{\phi})$ does *not* signal CP-violation, as it would in $(\phi-\bar{\phi})$.)

Appendix C: Spin-2

The spin-2 case shares many features with spin-1, including separate couplings to left and right chirality fields. We give the lagrangian for this case in Eq. 19. Once again, we parametrize the relative strengths of the chiral couplings with an angle ξ (Eq. B1). As mentioned in Section II, $q\bar{q}$ and gg production give rise to $J_{\text{beam}} = \pm 1$ and $J_{\text{beam}} = \pm 2$ spin states, respectively, and each proceed via dimension-five operators. We therefore should not prejudice one over the other in general, though gg production tends to benefit from higher parton luminosities in the case of lighter spin-2 resonances (less than about 2 TeV [23]), and $q\bar{q}$ for heavier resonances. The 5D angular distributions are

$$\frac{d^5\Gamma_{J_{\text{beam}}=\pm 2}}{d\Omega\, d\bar{\Omega}\, d\cos\Theta} \propto \big(1-\cos^4\Theta\big)\Big(1 - \cos\theta\cos\bar{\theta} + \sqrt{1-r^2}\cos(2\xi)\big(\cos\bar{\theta}-\cos\theta\big)\Big)$$

$$- \sin(2\xi) \sin^4 \Theta \sin\theta \sin\bar\theta \cos(\phi + \bar\phi)$$
$$+ r \Big[\cos\Theta \sin^3\Theta \big(1 + \sin(2\xi)\big) \big(\cos\theta \sin\bar\theta \cos\bar\phi + \cos\bar\theta \sin\theta \cos\phi \big)$$
$$- \sqrt{1 - r^2} \cos(2\xi) \cos\Theta \sin^3\Theta \big(\sin\bar\theta \cos\bar\phi - \sin\theta \cos\phi \big) \Big]$$
$$- r^2 \sin^2\Theta \Big[\cos^2\Theta - \sin(2\xi) - \big(1 - \sin(2\xi) \cos^2\Theta\big) \cos\theta \cos\bar\theta$$
$$+ \sin^2\Theta \sin\theta \sin\bar\theta \big(\cos\phi \cos\bar\phi + \sin(2\xi) \sin\phi \sin\bar\phi \big) \Big] \quad \text{(C1)}$$

and

$$\frac{d^5\Gamma_{J_{\text{beam}}=\pm 1}}{d\Omega \, d\bar\Omega \, d\cos\Theta} \propto \big(1 - 3\cos^2\Theta + 4\cos^4\Theta\big)\Big(1 - \cos\theta \cos\bar\theta$$
$$+ \sqrt{1 - r^2} \cos(2\xi)\big(\cos\bar\theta - \cos\theta\big)\Big)$$
$$+ \big(1 - 5\cos^2\Theta + 4\cos^4\Theta\big) \sin(2\xi) \sin\theta \sin\bar\theta \cos(\phi + \bar\phi)$$
$$+ \frac{1}{2} r \sin(4\Theta) \Big[\big(1 + \sin(2\xi)\big) \big(\cos\theta \sin\bar\theta \cos\bar\phi + \cos\bar\theta \sin\theta \cos\phi \big)$$
$$+ \sqrt{1 - r^2} \cos(2\xi) \big(\sin\theta \cos\phi - \sin\bar\theta \cos\bar\phi \big) \Big]$$
$$- \frac{1}{4} r^2 \Big[1 - 3\sin(2\xi) + 2\cos(4\Theta) + \big(1 - \sin(2\xi)\big) \cos(2\Theta)$$
$$- 2\cos\theta \cos\bar\theta \big[1 + \cos^2\Theta - \big(1 - 7\cos^2\Theta + 8\cos^4\Theta\big) \sin(2\xi)\big]$$
$$+ 2\sin^2\Theta \sin\theta \sin\bar\theta \Big(\big[1 - \sin(2\xi)\big(1 - 8\cos^2\Theta\big)\big] \sin\phi \sin\bar\phi$$
$$- \big[1 - 8\cos^2\Theta - \sin(2\xi)\big] \cos\phi \cos\bar\phi \Big) \Big]. \quad \text{(C2)}$$

Just as with spin-1, the $\cos\theta \cos\bar\theta$ distribution lets us distinguish in principle the difference between vector-like and axial-like couplings. For all spin-2 polarizations the relevant formulas are

$$\frac{d\Gamma_V}{d\cos\theta \, d\cos\bar\theta} \propto \Big(1 + \frac{2r^2}{3}\Big) - \Big(1 - \frac{2r^2}{3}\Big) \cos\theta \cos\bar\theta$$
$$\frac{d\Gamma_A}{d\cos\theta \, d\cos\bar\theta} \propto \big(1 - r^2\big)\big(1 - \cos\theta \cos\bar\theta\big), \quad \text{(C3)}$$

where V and A are respectively the cases of left-right symmetric and antisymmetric couplings. We see just a slight modification in the vector term compared to spin-1, but once again having $M \gtrsim 1$ TeV requires us to fit the distribution to within a few percent to discriminate between the two cases.

To avoid needing such precision and a full 2D parameter fit, we can integrate the lepton polar and production angles to find the distributions in $\phi, \bar\phi$. The leading term in r only depends on $\phi + \bar\phi$. We get

$$\frac{d\Gamma_{J_{\text{beam}}=P}}{d(\phi + \bar\phi)} \propto \Big(1 - \frac{1}{6} r^2 \big(1 - 5\sin(2\xi)\big)\Big) + \zeta_P \Big(\frac{\pi}{4}\Big)^2 \Big(\sin(2\xi) + \frac{1}{2} r^2 \big(1 - \sin(2\xi)\big)\Big) \cos(\phi + \bar\phi)$$
$$\frac{d\Gamma_{J_{\text{beam}}=P}}{d(\phi - \bar\phi)} \propto \Big(1 - \frac{1}{6} r^2 \big(1 - 5\sin(2\xi)\big)\Big) - \frac{1}{3} r^2 \Big(\frac{\pi}{4}\Big)^2 \big(1 + \sin(2\xi)\big) \cos(\phi - \bar\phi), \quad \text{(C4)}$$

where $\zeta_P = (-2/3,\ 1/6,\ 1)$ for $P = (\pm 2,\ \pm 1,\ 0)$, respectively. Once again, we see that the $(\phi - \bar{\phi})$-dependence is independent of resonance polarization (*cf.* discussion under Eq. B5).

The production of a spin-2 particle with $J_{\text{beam}} = 0$ requires an operator with dimension greater than five, *i.e.* beyond that of the other polarizations. It is for this reason that we did not list any equations for this state in Section II. However, we give here the differential decay rate with respect to leptonic and production angles, from which one can obtain the 0-polarization portion of Eq. C4,

$$
\begin{aligned}
\frac{d^5\Gamma_{J_{\text{beam}}=0}}{d\Omega\, d\bar{\Omega}\, d\cos\Theta} \propto\ & \sin^2(2\Theta)\Big(1 - \cos\theta\cos\bar{\theta} + \sin(2\xi)\sin\theta\sin\bar{\theta}\cos(\phi + \bar{\phi}) \\
& + \sqrt{1-r^2}\cos(2\xi)\sin^2(2\Theta)\big(\cos\bar{\theta} - \cos\theta\big)\Big) \\
& - \frac{1}{3}\, r\Big[\sin(2\Theta)\big(1 + 3\cos(2\Theta)\big)\big(1 + \sin(2\xi)\big)\big[\cos\theta\sin\bar{\theta}\cos\bar{\phi} + \cos\bar{\theta}\sin\theta\cos\phi\big] \\
& \qquad - \frac{1}{2}\sqrt{1-r^2}\cos(2\xi)\big(2\sin(2\Theta) + 3\sin(4\Theta)\big)\big(\sin\bar{\theta}\cos\bar{\phi} - \sin\theta\cos\phi\big)\Big] \\
& - r^2\Big[\sin^2 2\Theta\big(1 - \sin\theta\sin\bar{\theta}\cos\phi\cos\bar{\phi} + \sin(2\xi)(\cos\theta\cos\bar{\theta} - \sin\theta\sin\bar{\theta}\sin\phi\sin\bar{\phi})\big) \\
& \qquad - \frac{2}{9}\big(1 + \sin(2\xi)\big)\big(1 + 3\cos^2\Theta\big)\big(1 + \cos\theta\cos\bar{\theta} - \sin\theta\sin\bar{\theta}\cos(\phi - \bar{\phi})\big)\Big]. \quad \text{(C5)}
\end{aligned}
$$

[1] T. Aaltonen et al. (CDF), *Evidence for a Mass Dependent Forward-Backward Asymmetry in Top Quark Pair Production* (2011), 1101.0034.

[2] T. Aaltonen et al. (CDF), *Forward-Backward Asymmetry in Top Quark Production in $p\bar{p}$ Collisions at sqrts = 1.96 TeV*, Phys. Rev. Lett. **101**, 202001 (2008), 0806.2472.

[3] V. M. Abazov et al. (D0), *First Measurement of the Forward-Backward Charge Asymmetry in Top Quark Pair Production*, Phys. Rev. Lett. **100**, 142002 (2008), 0712.0851.

[4] The D0 Collaboration, *Measurement of the Forward-Backward Production Asymmetry of t and $\bar{t}$ Quarks in $p\bar{p} \to t\bar{t}$ Events* (2010), D0 Note 6062-CONF.

[5] The CDF Collaboration, *Measurement of the Forward-Backward Asymmetry in Top Pair Production in the Dilepton Decay Channel using 5.1 fb^{-1}* (2011), CDF Note 10436.

[6] P. H. Frampton, J. Shu, and K. Wang, *Axigluon as Possible Explanation for $p\bar{p} \to t\bar{t}$ Forward-Backward Asymmetry*, Phys. Lett. **B683**, 294 (2010), 0911.2955.

[7] J. C. Pati and A. Salam, *Mirror Fermions, J/psi Particles, Kolar Mine Events and Neutrino Anomaly*, Phys.Lett. **B58**, 333 (1975).

[8] L. J. Hall and A. E. Nelson, *Heavy Gluons and Monojets*, Phys. Lett. **B153**, 430 (1985).

[9] P. H. Frampton and S. L. Glashow, *Chiral Color: An Alternative to the Standard Model*, Phys. Lett. **B190**, 157 (1987).

[10] Y. Bai, J. L. Hewett, J. Kaplan, and T. G. Rizzo, *LHC Predictions from a Tevatron Anomaly in the Top Quark Forward-Backward Asymmetry* (2011), 1101.5203.

[11] J. L. Hewett, J. Shelton, M. Spannowsky, T. M. P. Tait, and M. Takeuchi, A_{FB}^t *Meets LHC* (2011), 1103.4618.

[12] C. Delaunay, O. Gedalia, Y. Hochberg, G. Perez, and Y. Soreq, *Implications of the CDF $t\bar{t}$ Forward-Backward Asymmetry for Hard Top Physics* (2011), 1103.2297.

[13] J. Aguilar-Saavedra and M. Perez-Victoria, *Probing the Tevatron $t\bar{t}$ Asymmetry at LHC*, JHEP **1105**, 034 (2011), 1103.2765.

[14] O. Antunano, J. H. Kuhn, and G. Rodrigo, *Top quarks, Axigluons and Charge Asymmetries at Hadron Colliders*, Phys. Rev. **D77**, 014003 (2008), 0709.1652.

[15] Y.-k. Wang, B. Xiao, and S.-h. Zhu, *One-side Forward-Backward Asymmetry in Top Quark Pair Production at CERN Large Hadron Collider*, Phys. Rev. **D82**, 094011 (2010), 1008.2685.

[16] Y.-k. Wang, B. Xiao, and S.-h. Zhu, *One-Side Forward-Backward Asymmetry at the LHC*, Phys. Rev. **D83**, 015002 (2011), 1011.1428.

[17] B. Xiao, Y.-K. Wang, Z.-Q. Zhou, and S.-h. Zhu, *Edge Charge Asymmetry in Top Pair Production at the LHC*, Phys.Rev. **D83**, 057503 (2011), 1101.2507.

[18] D. Choudhury, R. M. Godbole, R. K. Singh, and K. Wagh, *Top Production at the Tevatron/LHC and Nonstandard, Strongly Interacting Spin one Particles*, Phys. Lett. **B657**, 69 (2007), 0705.1499.

[19] R. M. Godbole, K. Rao, S. D. Rindani, and R. K. Singh, *On Measurement of Top Polarization as a Probe of $t\bar{t}$ Production Mechanisms at the LHC*, JHEP **11**, 144 (2010), 1010.1458.

[20] C. Degrande, J.-M. Gerard, C. Grojean, F. Maltoni, and G. Servant, *Non-resonant New Physics in Top Pair Production at Hadron Colliders* (2010), 1010.6304.

[21] J. Cao, L. Wu, and J. M. Yang, *New Physics Effects on Top Quark Spin Correlation and Polarization at the LHC: A Comparative Study in Different Models* (2010), 1011.5564.

[22] D.-W. Jung, P. Ko, and J. S. Lee, *Longitudinal Top Polarization as a Probe of a Possible Origin of Forward-Backward Asymmetry of the Top Quark at the Tevatron* (2010), 1011.5976.

[23] R. Frederix and F. Maltoni, *Top Pair Invariant Mass Distribution: A Window on New Physics*, JHEP **01**, 047 (2009), 0712.2355.

[24] W. Bernreuther, A. Brandenburg, Z. Si, and P. Uwer, *Top Quark Pair Production and Decay at Hadron Colliders*, Nucl.Phys. **B690**, 81 (2004), hep-ph/0403035.

[25] K. Agashe, A. Belyaev, T. Krupovnickas, G. Perez, and J. Virzi, *LHC Signals from Warped Extra Dimensions*, Phys. Rev. **D77**, 015003 (2008), hep-ph/0612015.

[26] L. G. Almeida, S. J. Lee, G. Perez, I. Sung, and J. Virzi, *Top Jets at the LHC*, Phys.Rev. **D79**, 074012 (2009), 0810.0934.

[27] J. Shelton, *Polarized Tops from New Physics: Signals and Observables*, Phys. Rev. **D79**, 014032 (2009), 0811.0569.

[28] D. Krohn, J. Shelton, and L.-T. Wang, *Measuring the Polarization of Boosted Hadronic Tops* (2009), 0909.3855.

[29] V. D. Barger, J. Ohnemus, and R. J. N. Phillips, *Spin Correlation Effects in the Hadroproduction and Decay of Very Heavy Top Quark Pairs*, Int. J. Mod. Phys. **A4**, 617 (1989).

[30] Y. Hara, *Angular Correlation of Charged Leptons from $t\bar{t}$ Produced in the Gluon Fusion*, Prog.Theor.Phys. **86**, 779 (1991), revised version.

[31] G. L. Kane, G. Ladinsky, and C. Yuan, *Using the Top Quark for Testing Standard Model Polarization and CP Predictions*, Phys.Rev. **D45**, 124 (1992).

[32] G. Mahlon and S. J. Parke, *Angular Correlations in Top Quark Pair Production and Decay at Hadron Colliders*, Phys.Rev. **D53**, 4886 (1996), hep-ph/9512264.

[33] T. Stelzer and S. Willenbrock, *Spin Correlation in Top Quark Production at Hadron Colliders*, Phys.Lett. **B374**, 169 (1996), hep-ph/9512292.

[34] G. Mahlon and S. J. Parke, *Spin Correlation Effects in Top Quark Pair Production at the LHC*, Phys.Rev. **D81**, 074024 (2010), 1001.3422.

[35] M. Beneke, I. Efthymiopoulos, M. L. Mangano, J. Womersley, A. Ahmadov, et al., *Top Quark Physics* (2000), hep-ph/0003033.

[36] J. Bernabeu, N. Rius, and A. Pich, *Tau Spin Correlations at the Z peak: Aplanarities of the Decay Products*, Phys. Lett. **B257**, 219 (1991).

[37] R. Barate et al. (ALEPH), *Measurement of the Transverse Spin Correlations in the Decay $Z \to \tau^+\tau^-$*, Phys. Lett. **B405**, 191 (1997).

[38] P. Abreu et al. (DELPHI), *Measurement of the Transverse Spin Correlation in $Z \to \tau^+\tau^-$ Decays*, Phys. Lett. **B404**, 194 (1997).

[39] R. Volkert, *A Full Spin Analysis of the Process $e^+e^- \to \tau^+\tau^-$ using the L3 Detector at LEP*

(1997), DESY-ZEUTHEN-97-04.

[40] M. R. Buckley, H. Murayama, W. Klemm, and V. Rentala, *Discriminating Spin Through Quantum Interference*, Phys.Rev. **D78**, 014028 (2008), 0711.0364.

[41] M. R. Buckley, B. Heinemann, W. Klemm, and H. Murayama, *Quantum Interference Effects Among Helicities at LEP-II and Tevatron*, Phys.Rev. **D77**, 113017 (2008), 0804.0476.

[42] M. R. Buckley, S. Y. Choi, K. Mawatari, and H. Murayama, *Determining Spin through Quantum Azimuthal-Angle Correlations*, Phys.Lett. **B672**, 275 (2009), 0811.3030.

[43] H. Murayama and V. Rentala, *Randall-Sundrum Graviton Spin Determination using Azimuthal Angular Dependence* (2009), 0904.4561.

[44] F. Boudjema and R. K. Singh, *A Model Independent Spin Analysis of Fundamental Particles Using Azimuthal Asymmetries*, JHEP **0907**, 028 (2009), 0903.4705.

[45] Y. Kiyo, J. Kodaira, and K. Morii, *Azimuthal Angular Dependence of Decay Lepton in $e^+e^- \to t\bar{t}$*, Eur.Phys.J. **C18**, 327 (2000), hep-ph/0008065.

[46] W. Bernreuther, M. Flesch, and P. Haberl, *Signatures of Higgs bosons in the Top Quark Decay Channel at Hadron Colliders*, Phys. Rev. **D58**, 114031 (1998), hep-ph/9709284.

[47] W. Bernreuther, A. Brandenburg, and M. Flesch, *Effects of Higgs Sector CP Violation in Top Quark Pair Production at the LHC* (1998), hep-ph/9812387.

[48] J. Gallicchio, J. Huth, M. Kagan, M. D. Schwartz, K. Black, et al., *Comprehensive Multivariate Discrimination and the Higgs + W/Z search* (2010), 1010.3698.

[49] A. Brandenburg, Z. G. Si, and P. Uwer, *QCD-corrected Spin Analysing Power of Jets in Decays of Polarized Top Quarks*, Phys. Lett. **B539**, 235 (2002), hep-ph/0205023.

[50] Y. Gao, A. V. Gritsan, Z. Guo, K. Melnikov, M. Schulze, et al., *Spin Determination of Single-Produced Resonances at Hadron Colliders*, Phys.Rev. **D81**, 075022 (2010), 1001.3396.

[51] K. Melnikov and M. Schulze, *Top Quark Spin Correlations at the Tevatron and the LHC* (2011), 1103.2122.

[52] Y. Bai and Z. Han, *Top-Antitop and Top-Top Resonances in the Dilepton Channel at the CERN LHC*, JHEP **0904**, 056 (2009), 0809.4487.

[53] L. Landau, Dokl. Akad. Nawk (USSR) **60**, 207 (1948).

[54] C.-N. Yang, *Selection Rules for the Dematerialization of a Particle Into Two Photons*, Phys.Rev. **77**, 242 (1950).

[55] J. Alwall et al., *MadGraph/MadEvent v4: The New Web Generation*, JHEP **09**, 028 (2007),

0706.2334.

[56] T. Sjostrand, S. Mrenna, and P. Skands, *PYTHIA 6.4 Physics and Manual*, JHEP **05**, 026 (2006), hep-ph/0603175.

[57] M. Cacciari and G. P. Salam, *Dispelling the N^3 Myth for the k_t Jet-Finder*, Phys. Lett. **B641**, 57 (2006), hep-ph/0512210.

[58] K. Rehermann and B. Tweedie, *Efficient Identification of Boosted Semileptonic Top Quarks at the LHC* (2010), 1007.2221.

[59] ATLAS Collaboration, *Prospects for Early $t\bar{t}$ Resonance Searches in ATLAS* (2009), ATL-PHYS-PUB-2010-008.

[60] J. Thaler and L.-T. Wang, *Strategies to Identify Boosted Tops*, JHEP **07**, 092 (2008), 0806.0023.

[61] ATLAS Collaboration, *Reconstruction of High Mass $t\bar{t}$ Resonances in the Lepton+Jets Channel* (2009), ATL-PHYS-PUB-2009-81.

[62] M. Cacciari, G. P. Salam, and G. Soyez, *The Anti-k_t Jet Clustering Algorithm*, JHEP **04**, 063 (2008), 0802.1189.

[63] L. Sonnenschein, *Analytical Solution of $t\bar{t}$ Dilepton Equations*, Phys. Rev. **D73**, 054015 (2006), hep-ph/0603011.

[64] A. A. Affolder et al. (CDF), *Measurement of the Top Quark Mass with the Collider Detector at Fermilab*, Phys. Rev. **D63**, 032003 (2001), hep-ex/0006028.

[65] U. Baur and L. H. Orr, *High p_T Top Quarks at the Large Hadron Collider*, Phys. Rev. **D76**, 094012 (2007), 0707.2066.

[66] P. Konar, K. Kong, and K. T. Matchev, *$\sqrt{\hat{s}}_{min}$: A Global Inclusive Variable for Determining the Mass Scale of New Physics in Events with Missing Energy at Hadron Colliders*, JHEP **03**, 085 (2009), 0812.1042.

[67] P. Konar, K. Kong, K. T. Matchev, and M. Park, *RECO Level $\sqrt{s}_{min}$ and Subsystem $\sqrt{s}_{min}$: Improved Global Inclusive Variables for Measuring the New Physics Mass Scale in Missing Energy Events at Hadron Colliders* (2010), 1006.0653.

[68] H. Davoudiasl, S. Gopalakrishna, and A. Soni, *Big Signals of Little Randall-Sundrum Models* (2009), 0908.1131.

[69] J. C. Collins and D. E. Soper, *Angular Distribution of Dileptons in High-Energy Hadron Collisions*, Phys. Rev. **D16**, 2219 (1977).

[70] G. Brooijmans, *High pT Hadronic Top Quark Identification. Part I: Jet Mass and YSplitter* (2008), ATL-PHYS-CONF-2008-008.

[71] D. E. Kaplan, K. Rehermann, M. D. Schwartz, and B. Tweedie, *Top Tagging: A Method for Identifying Boosted Hadronically Decaying Top Quarks*, Phys. Rev. Lett. **101**, 142001 (2008), 0806.0848.

[72] L. G. Almeida, S. J. Lee, G. Perez, G. F. Sterman, I. Sung, et al., *Substructure of High-pT Jets at the LHC*, Phys.Rev. **D79**, 074017 (2009), 0807.0234.

[73] L. G. Almeida, S. J. Lee, G. Perez, G. Sterman, and I. Sung, *Template Overlap Method for Massive Jets*, Phys.Rev. **D82**, 054034 (2010), 1006.2035.

[74] T. Plehn, M. Spannowsky, M. Takeuchi, and D. Zerwas, *Stop Reconstruction with Tagged Tops* (2010), 1006.2833.

[75] S. D. Ellis, C. K. Vermilion, and J. R. Walsh, *Techniques for Improved Heavy Particle Searches with Jet Substructure*, Phys. Rev. **D80**, 051501 (2009), 0903.5081.

[76] J. Thaler and K. Van Tilburg, *Identifying Boosted Objects with N-subjettiness*, JHEP **03**, 015 (2011), 1011.2268.

[77] A. Abdesselam, E. Kuutmann, U. Bitenc, G. Brooijmans, J. Butterworth, et al., *Boosted Objects: A Probe of Beyond the Standard Model Physics*, Eur.Phys.J.C (2010), 1012.5412.

[78] T. Aaltonen et al. (CDF), *First Measurement of the $t\bar{t}$ Differential Cross Section $d\sigma/dM_{t\bar{t}}$ in $p\bar{p}$ Collisions at $\sqrt{s} = 1.96$ TeV*, Phys. Rev. Lett. **102**, 222003 (2009), 0903.2850.

[79] V. M. Abazov et al. (D0), *Search for $t\bar{t}$ Resonances in the Lepton Plus Jets Final State in $p\bar{p}$ Collisions at $\sqrt{s} = 1.96$ TeV*, Phys. Lett. **B668**, 98 (2008), 0804.3664.

[80] The ATLAS Collaboration, *Search for New Physics in Dijet Mass and Angular Distributions in pp Collisions at $\sqrt{s} = 7$ TeV Measured with the ATLAS Detector* (2011), 1103.3864.

[81] The CMS Collaboration, *Measurement of Dijet Angular Distributions and Search for Quark Compositeness in pp Collisions at 7 TeV* (2011), 1102.2020.

[82] The CMS Collaboration, *Search for Resonances in Semi-leptonic Top-pair Decays Close to Production Threshold* (2011), CMS PAS TOP-10-007.

[83] W. Bernreuther and Z.-G. Si, *Distributions and Correlations for Top Quark Pair Production and Decay at the Tevatron and LHC*, Nucl. Phys. **B837**, 90 (2010), 1003.3926.

[84] K. Melnikov and M. Schulze, *NLO QCD Corrections to Top Quark Pair Production and Decay at Hadron Colliders*, JHEP **08**, 049 (2009), 0907.3090.

[85] K. Melnikov and M. Schulze, *NLO QCD Corrections to Top Quark Pair Production in Association with one Hard Jet at Hadron Colliders*, Nucl. Phys. **B840**, 129 (2010), 1004.3284.